Metal Filament 3D Printing of SS316L- Focusing on the printing process

Karthikesh Gante Lokesha Renukaradhya

KTH ROYAL INSTITUTE OF TECHNOLOGY
SCHOOL OF INDUSTRIAL ENGINEERING AND MANAGEMENT

Royal Institute of Technology

Master Thesis

MF223X

Experimental Work with 3D Printing
of SS316L Metal Filament

Author:

Karthikesh Gante Lokesha Renukaradhya

Supervisor:

Pasi Kangas
Susanne Norgren
Amir Rashid

Examiner:

Ulf Sellgren

JANUARY 21, 2019

Abstract

As a cutting edge manufacturing methodology, 3D printing or additive manufacturing (AM) brings much more attention to the fabrication of complex structure, especially in the manufacturing of metal parts.A number of various metal AM techniques have been studied and commercialized. However, most of them are expensive and less available, in comparison with Selective Laser Melting manufactured stainless steel 316L component.The purpose of this Master Thesis is to introduce an innovative AM technique which focuses on material extrusion-based 3D printing process for creating a Stainless Steel 316L part using a metal-polymer composite filament. The Stainless Steel test specimen was printed using an Fused Deposition Modelling based 3D printer loaded with a metal infused filament, followed by industrial standard debinding and sintering process. Investigation was performed on the specimen to understand the material properties and their behaviour during the post-processing method. In addition effects of debinding, sintering and comparison of the test Specimen before and after debinding stages was also carried out. Metal polymer filaments for 3D printing could be an alternative way of making metal AM parts.

Keywords

Additive manufacturing, stainless steel 316L, metal-polymer, sintering, Post processing, 3D printer.

Examensarbete TRITA-ITM-EX 2019:592		
Metal Filament 3D Printing of SS316L-Fokuserar på printing processen		
Karthikesh Gante Lokesha Renukaradhya		
Godkänd 2019-09-11	Examinator Ulf Sellgren, KTH	Handledare Amir Rashid, KTH
	Uppdragsgivare Sandvik Group	Kontaktperson Pasi Kangas, Sandvik Group

Sammanfattning

Som en avancerad tillverkningsmetodik ger 3D-printing eller additiv tillverkning (AM) mycket mer uppmärksamhet vid tillverkning av komplex struktur, särskilt vid tillverkning av metallkomponenter. Ett antal olika AM-tekniker vid tillverkningen av olika typer av metallkomponenter har studerats och kommersialiserats.De flesta av dessa AM-tekniker är dyra och mindre tillgängliga, i jämförelse med Selective Laser Melting vid tillverkningen av en komponent i rostfritt stål 316L. Syftet med detta examensarbete är att introducera en innovativ AM-teknik som fokuserar på materialsträngsprutningsbaserad 3D-printingprocess för att skapa ekomponent i rostfritt stål 316L-komponent med ett metallpolymerkompositfilament. Ett prov bestående av rostfritt stål skrevs ut med en FDM-baserad 3D-skrivare laddad med filament av polymer och metal, följt av industriell avdrivnings-och sintringsprocess. Provet studerades för att förstå materialegenskaperna och dess beteende under efterbehandlingsmetoden. Dessutom genomfördes också resultat från avdrivning och sintring på provet och en jämförelse av provet före och efter avdrivnlngssteget. Metallpolymertrådar för 3D-printing kan vara ett alternativt sätt att tillverka AM-metallkomponenter.

Nyckelord

Additiv tillverkning, rostfritt stål 316L, metallpolymer, sintring.

Acknowledgement

Abbreviations

AM	Additive Manufacturing.
CAD	Computer Aided Design.
FDM	Fused Deposition Modelling
SLM	Selective Laser Melting
STL	Stereolithography
LOM	Laminated object manufacturing
3DP	3D printing
LENS	Laminated engineered net shaping
EBM	Electron beam melting
BJ	Binder Jet
FFF	Fused Filament Fabrication
MIM	Metal Injection Moulding

Contents

List of Figures

List of Tables

1 SANDVIK

This Master Thesis was carried out at the division for Additive Manufacturing (AM) at Sandvik. The industrial company has a global profile focusing on engineering tools for mining, equipment and tooling systems for metal cutting. The advanced stainless steel, special alloys and products for industrial heating are other core areas. Sandvik has three RD/sales service business areas: Sandvik Materials Technology, Sandvik Mining Rock Technology and Sandvik Machining Solutions. The division for AM is part of the Sandvik Machining Solutions[5]. The company was founded in 1862 by Goran Fredrik Goransson. The focus on high quality and added value, operating, investing in R & D and close customer service led to successful business[20]. Nowadays, Sandvik has developed a worldwide brand with new and innovative techniques such as AM. The research centre for AM was established in 2014 in Sandviken to develop new possibilities of manufacturing complex geometries, which may benefit in comparison to a more traditional production approach.

2 INTRODUCTION

3D printing, fundamentally known as additive manufacturing (AM) is a process where products are constantly built layer by layer through computer-aided controlled operations. A virtual model is first designed with relevant computer-aided design (CAD) software, then translated into standard tessellation language (.stl) electronic data understandable by the printer. This electronic data is then used to control the motion and trajectory of the printing head fitted with a focused heat source. This selectively melts and consolidates commonly used feedstock material (usually in powder or filament form) to create 3D parts.3D printing provides real-time rapid prototyping of product models making it possible to visualize the design prior to actual production. These virtual manufacturing techniques speed up design iterations and allow designers, researchers, and manufacturers to generate prototypes within the shortest time possible. In addition they can obtain feedbacks and refine designs through early error detection and correction.

3D printed components offer a high degree of geometrical flexibility and accuracy without almost any loss of material.This leads to resource savings and eco-design optimization.This novel manufacturing technology produces not only functional research prototypes to enhance product quality, process parameters, and material universalisation during the design process but also full-scale components for actual applications.

2.1 Background

The history of additive manufacturing dates back to the late 19th century in the fields of topography and photo sculpture [5].Although experiments occurred as far back as the 1960s in the photo-glyph recording technique that selectively exposed layers of a transparent photo emulsion while scanning cross-sections of the object to be replicated [20]it was not until 1983 when pioneers Charles Hull (founder of 3D Systems) and Scott Crump (founder of Stratasys) developed modern-day range of technologies now known as 3D printing[16].They worked on additive processes such as Stereolithography (SLA) and selective laser sintering (SLS) that created solid objects layer by layer using 3D CAD data and ultraviolet light to cure photo polymeric resins. As the processes evolved, they became known as additive manufacturing (AM) [6].Additive manufacturing began with a limited set of processes and materials with a primary goal of producing prototypes. However, the early 1990s saw an era of spontaneous emergence of new AM technologies and materials. Fast forward to date, sophisticated AM technologies have been developed and extensive research on materials is being conducted [12].In addition, the focus has shifted from prototyping to fabrication of full-scale functional parts [5].Figure 2.1 illustrates the progressive developments in AM technologies and materials that have taken place through time.
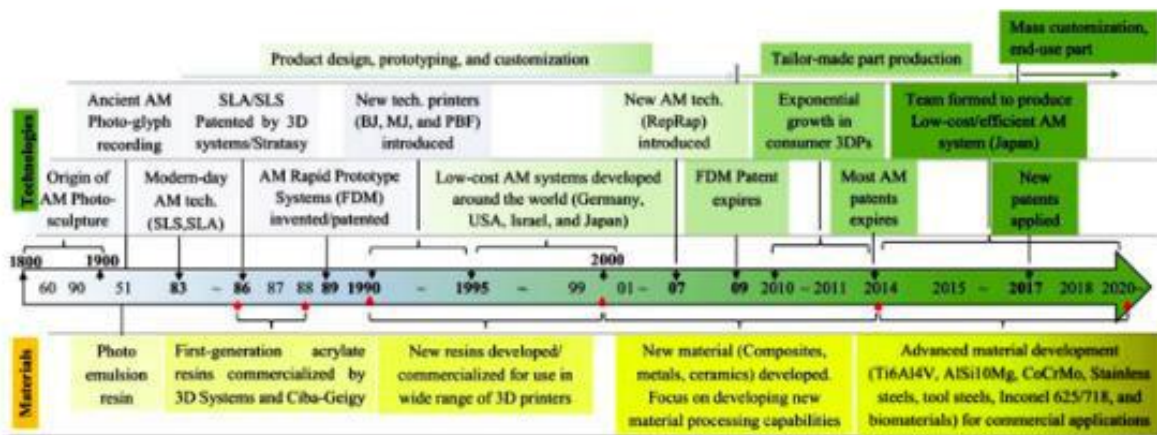
Figure 2.1: Progressive development in AM technologies and material
[5]

With rapid prototyping, scientists and students can rapidly build and analyze models for theoretical comprehension and studies. Doctors can build a model of a damaged body to analyze it and plan better the procedure, market researchers can see what people think of a particular new product, and rapid prototyping makes it easier for artists to explore their creativity

The steps involved in product development using rapid prototyping are shown in figure 2.2.Here, it can be seen that creating models faster save a lot of time and there is the possibility of testing more models.[3, 12]
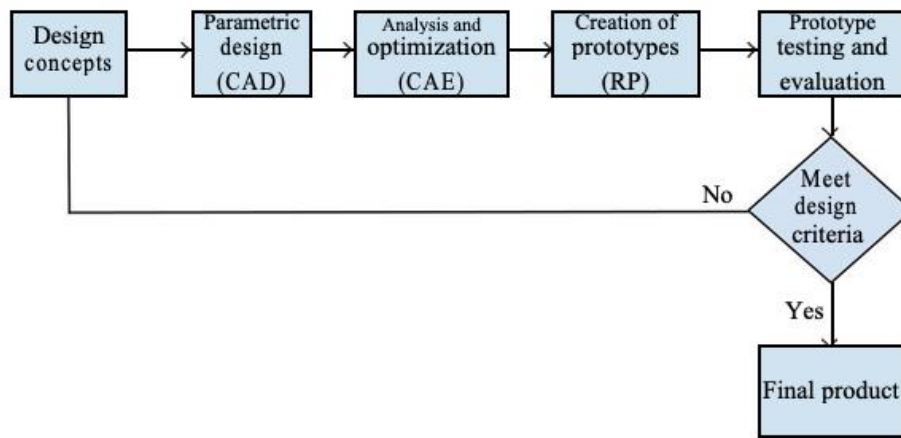
Figure 2.2: Product development cycle
[3]

Furthermore, different kind of materials can be applied in the AM process depending on the type of product and manufacturing process.Polymers, ceramics and metals are different materials that can be integrated into the AM process[11]. In Figure 2.3,there is an overview of the different additive manufacturing processes that are illustrated.The criterion used is to classify these processes into a liquid base, solid-based, and powder-based.
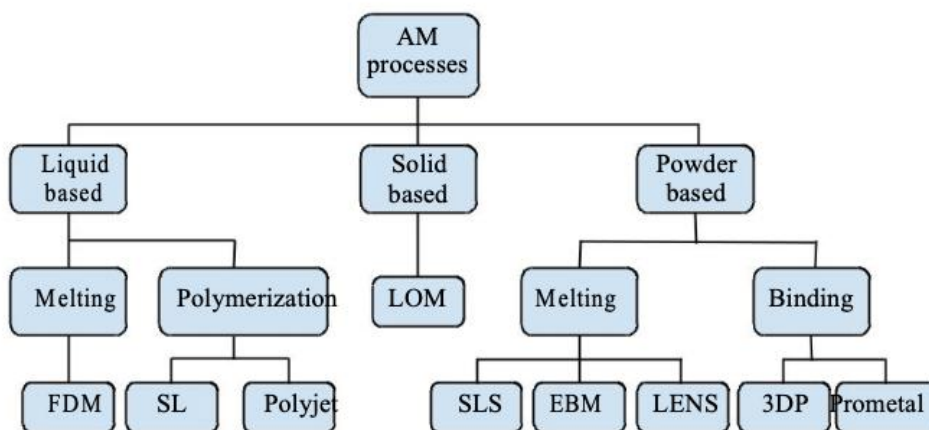
Figure 2.3: An overview of the AM process depending on the material
[11]

The processes included in this review are considered the most relevant in the past and promising for the future of the industry. The processes considered are stereolithography (SLA), Polyjet, fused deposition modelling (FDM), laminated object manufacturing (LOM), 3D printing (3DP), Prometal, selective laser sintering (SLS), laminated engineered net shaping (LENS), and (EBM). The liquid-and powder-based pro-cesses seem more promising than solid-based processes of which LOM is the predominant one today. In 2004 ,EBM, Prometal, LENS, and Polyjet were non-existent.[10]

2.2 Aim

This Thesis work aims to assess and discuss the FDM technique in its entire set from the different composition of stainless steel 316L metal filament used to the printing of the green part, allowing understanding what are the benefits and limitation of metal FDM process towards conventional manufacturing process. In order to perform such a task, two comparisons were performed: at a technical level and another one at the material level. In the technical level, FDM was compared to the typical polymer processing technique, which acts as the reference technique for the study. In the material level, commercially available Stainless steel 316L metal filaments with different metal to polymer densities were purchased and used in an FDM printer.

In this work, to reduce the amount of parameters a filament from virtual foundry having 83% metal density and a Prusa 3D printer was selected. Also in this thesis work we have studied the impact of printing temperatures, nozzle type, printing patters and adhesion between layers.

2.3 Research Question

Based on the aim of this study, the following problem statements are defined to execute this thesis:

- Is it possible to print a green body using the SS316L metal-polymer filament in a plastic printing 3D printer?

- What print parameters shall be used for SS316L filament in order to achieve a rigid green body after printing?

2.4 Delimitation

As this project aim to discuss and evaluate a new innovative metal 3D printing process and also to understand how different parameters are required to produce a metal part, all the major possible factors are considered. But still there are few that were not considered for this thesis work.

- The produced 3D printed metal parts are not considered for any industrial application.

- The density of the green body as well as the post processed metal part are not considered.

3 ADDITIVE MANUFACTURING

3.1 Literature Survey-Fused Deposition Modelling

Fused deposition modelling (FDM) is a additive manufacturing (AM) technology that is used to generate unique products from technically developed CAD models. Special design software is used to design and transfer point cloud data to a 3D printer. The process entails a collection of settings including speed, size, support, material, and quality control which must be set to ensure desired output is realized. Based on the process parameters selected, the digital model is translated into line-by-line printer instructions often termed as the G-code. The electronic data (G-code) control the toolpath, position, and speed thereby ensuring the execution of predetermined motions. The material usually in filament form is conveyed from a reel to the preheated nozzle by motorized gears. It is then heated to some temperatures slightly above the melting point and immediately deposited onto the build platform. Once a layer is completed, the build platform is moved a unit layer distance downwards and a subsequent layer laid. This process is repeated layer after layer until the entire product is completed. Since the material undergoes repeated heating and cooling, it is important to select a material that is capable of withstanding these complicated thermal variations.3D printing can produce prototypes and end-use parts with intricate geometries that are difficult or impossible to manufacture by conventional methods at reduced cycle time, inventory, and cost[13].

A literature paper by Carlo Burkhardt[1] primarily focuses on the process of fused filament fabrication a commercially predominant additive manufacturing technology an alternative to the MIM process. A popular technology worldwide has several advantages when compared to other AM techniques. The work provides a brief on the experimental process for printing on a tailored FFF machine using specific properties of sintered 316L steel parts. This technology typically uses a filament made of thermoplastic material feed, which eliminates the possibility of using a conventional metal injection moulding feedstock. This feedstock filament exhibited suitable viscosity and mechanical properties however had a higher temperature conductivity which resulted in the modification of print head and notable scrutiny given to temperature distribution during the shaping process of the metallic parts with higher geometrical accuracy. Solvent debinding the main binder was removed using the debinding agent cyclohexane and subsequent drying in ambient conditions. Thermal debinding and sintering were carried out in a combined run but this process, however, led to parts with high density but with geometry distortion. Additionally, the printing lines were found not to disappear in the sintering process causing high surface roughness and regularly structured open porosity which thus required optimization of printing parameters.

According to the author when compared, the green parts formed via FFF to that of MIM, we see uniform grain size distribution, but with larger pores near the surface in the FFF process, probably due to lower forming pressure applied during printing compared to the latter. Investigations were carried out on three different post treatment methods: grinding, sandblasting and laser structuring. Amidst the three different post treatment techniques which have been investigated, laser polishing/structuring was found to be more feasible, with the emergence of surfaces with good properties. To draw conclusions, this literature presents a state of the artwork being carried out in the field of additive manufacturing methodology where Fused Filament fabrication proves to be a promising technology for metals with complex microstructures. Additionally, FFF technology proves to have an edge over other methodologies, in terms of simple and effortless change of material. The tailored Fused Filament Fabrication allows printing green parts out of 316L stainless steel feedstock effortlessly, however, the surface properties obtained were not found to be satisfactory for the surface critical applications without after treatment. Scope for further research could possibly be a combination of green part printing and surface polishing procedure in one print head.

3.2 Introduction to Fused Deposition Modelling
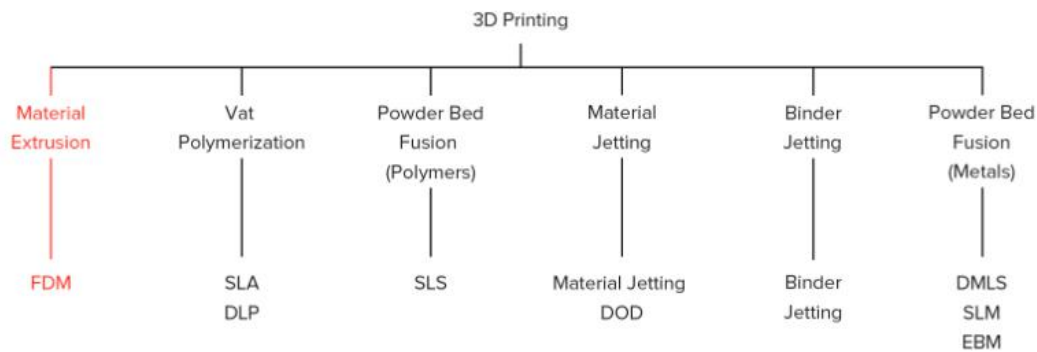
Figure 3.1: An overview of Different AM Techniques
[19]

Fused Deposition Modeling (FDM), or Fused Filament Fabrication (FFF), is an additive manufacturing process that belongs to the material extrusion family. In FDM, an object is built by selectively depositing melted material in a pre-determined path layer-by-layer. The materials used are thermoplastic polymers and come in a filament form.

FDM is the most widely used 3D printing technology for plastics: it represents the largest installed base of 3D printers globally and is often the first technology people are exposed to. In this article, the basic principles and the key aspects of the technology are presented. A designer should keep in mind the capabilities and limitations of the technology when fabricating a part with FDM, as this will help him to achieve the best result[19].

Among the different available additive manufacturing techniques discussed before the FDM process is the most popular one. Presently FDM process is showing the higher potential for product manufacturing with the potential to correlate with conventional polymer processing technique. Nevertheless, the scope of metal filament available for FDM is limited and costly, which hampers the use of this technique for manufacturing the final product. Neither the material nor the process has been studied in an efficient manner towards component production. However, the published studied until now the extrusion processing used in the production of filament with suitable filament diameter for the FDM process. This relevant information will be helpful for the development of new filament material for FDM and also for the use of this technique into the production of the final product. The optimization of filament production could escalate their properties and provide broad information on the process. The literature lacks studies and paper for metal FDM technique from the filament production, allowing complete control of the process and appropriate comparison between different AM techniques.

3.3 How does Fused Deposition Modelling Work
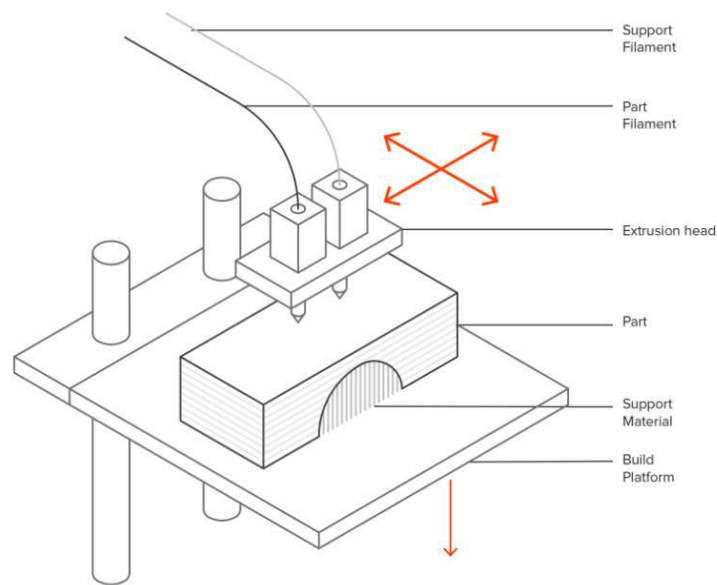
Figure 3.2: Schematic of a typical FDM printer
[19]

Here is how the FDM fabrication process works:

- A spool of thermoplastic filament is first loaded into the printer. Once the nozzle has reached the desired temperature, the filament is fed to the extrusion head and in the nozzle where it melts.

- The extrusion head is attached to a 3-axis system that allows it to move in the X, Y and Z directions. The melted material is extruded in thin strands and is deposited layer-by-layer in predetermined locations, where it cools and solidifies. Sometimes the cooling of the material is accelerated through the use of cooling fans attached on the extrusion head.

- To fill an area, multiple passes are required (similar to colouring a rectangle with a marker). When a layer is finished, the build platform moves down (or in other machine setups, the extrusion head moves up) and a new layer is deposited. This process is repeated until the part is complete.[19]

3.4   The FDM Process

The fused deposition modelling is a rapid prototyping process as illustrated in figure3.3. The three-axis motion coordinates system moves the extruder in x-y-z-direction while extruding a specific amount of material. The driver gear used in the FDM printer engages the filament and forces it through a thermistor-regulated heating block and nozzle. This produces a strand of molten material out of the nozzle which is deposited in layers and subsequently cooled to an FDM part. During this process for each layer, both the outer parameter and the solid infill are extruded.[17]
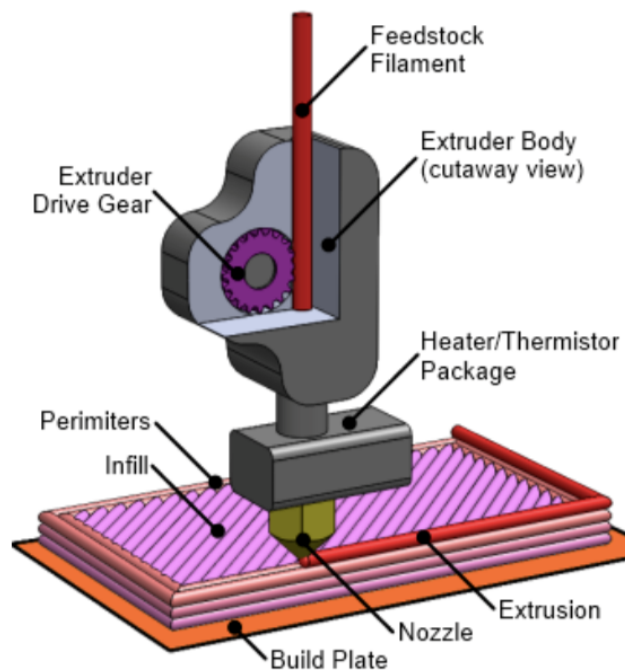
Figure 3.3: Illustration of Basic Hardware system for FDM 3D Printing
[17]

The infill is typically a pattern in the areas of the layer which correlates to the inside of the part being produced.The corresponding distance between the nozzle and the build plate is adjusted in a fixed increment between the building of the layers.The final setting of the print file defines towards which end of the printing range one looks: if towards the geometric resolution or mechanical performance.For a better understanding of the print quality, Figure 3.4 illustrates the influence of feeding rate and linear moment speed for a given layer height on the extrusion width.Increase in the feeding rate leads to an increase in the extrusion width.
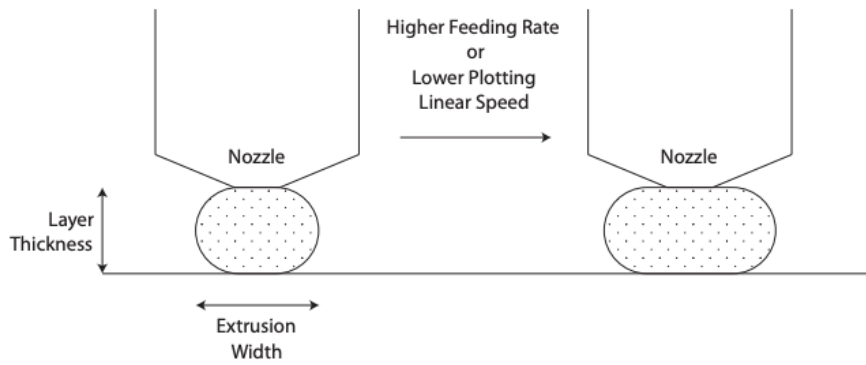
Figure 3.4: Illustration of FDM width Extrusion Parameter
[2]

FDM process is a straightforward technique that provides the advantages of being a highly reliable process, which requires low initial investment and also uses of relatively low-cost material. It is friendly to be operated in an office environment with short build time for parts with thin walls and low material waste. On the other hand, the material used in the FDM process must have lower melting temperature and if the part requires support then they will lead to poor surface finish.[2]

3.5 FDM Process Break-Down

Typically, the mechanical aspects of FDM are managed by the 3D printer hardware and software. Hence it becomes necessary to generate a suitable toolpath which allows the production of the part in an efficient and timely manner. The software which is used to produce the required toolpath procedure is illustrated in figure 3.5.The initial stage is the generation of a 3D model from designing software such as a computer-aided drawing CAD or importing 3D scan geometry.

The next step in the process is the conversion of the 3D model into a mesh file which is implemented in the stereolithography(STL) format[17]. Following this step is the splitting up of the mesh structure into layers and producing the tool path by using a program called slicer. The final step in this process is the use of machine control software to feed the data into the 3d printer to produce the required part. The steps followed to generate the 3D model in figure 3.5 rely on a number of important parameters which have been explained in detail in the next chapter.
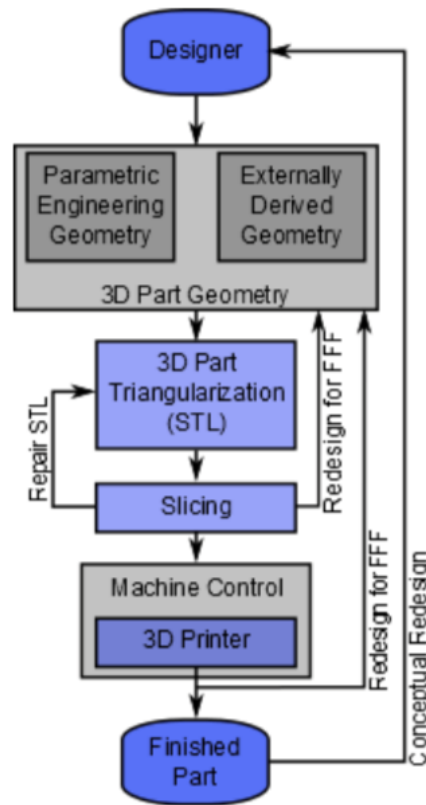
Figure 3.5: The FDM Process which is broken down into different stages
[17]

3.6   Design For FDM

One of the major strengths of the FDM process is that they do not demand huge design for manufacturing requirements, and facilitate the manufacturing of difficult, expensive parts which are difficult to produce by conventional means.However, there are many design practices which may be considered to produce a part form FDM process in a cost and time-effective manner[17].In the following chapter, we discuss various practices which give insight into the tuning of the parameters mentioned in the previous section.

3.6.1   Infill

To minimize the use of the material in the FDM process the parts are usually from a solid outer perimeter shell but has an inside infill pattern. This perimeter and infill are generated using the program called slicer. Several parameters are given in table7.1 can be adjusted to produce to a decent part. With an increase infill density, both the mechanical strength and production cost will increase proportionately.In this study for the stainless steel 316L filament, a complete 100% infill density was used.The internal geometry with different infill density are as shown below in figure3.6a.
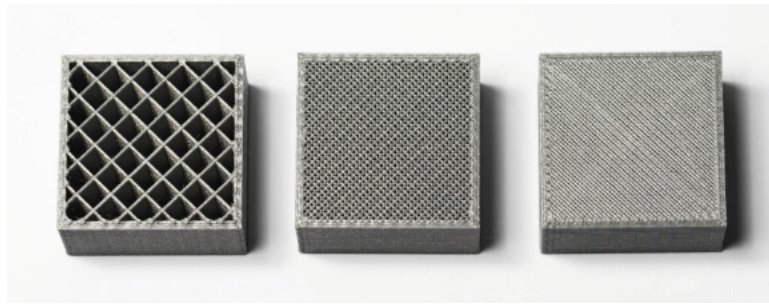
(a)
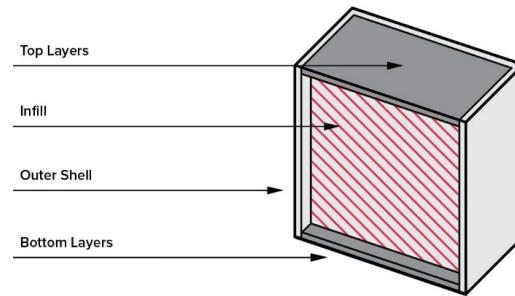
(b)

Figure 3.6: The internal geometry of the printed part with different infill density [19]
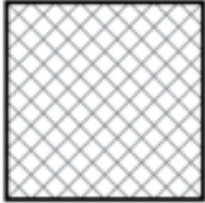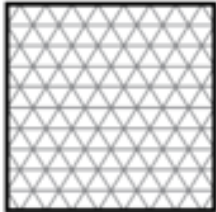
The infill is commonly composed of either rectilinear or hexagonal pattern as illustrated in figure 3.7. Generally, we prefer to use rectilinear infill patterns in this experiment because of two main reasons. First, a rectilinear infill pattern is simple to compute which results in less printing time. Secondly, a rectilinear pattern allows the relative orientation of the infill strands to be adjusted along with the mechanical properties of the part.[17]

Figure 3.7: Hexagonal (top) compared to rectangular (bottom) infill pattern [17]

The most common infill shapes are :

INFILL GEOMETRY	DESCRIPTION
	Rectangular-This is one of the most common and infill used in FDM prints. This pattern has strength in all directions and is quick to print.
	Honeycomb-This is one of the popular infill patterns used in FDM printing. It is quick to print and provides good strength in all directions.
	Triangular-This infill pattern is used when a good strength is needed in the direction of the walls. It consumes longer printing time.

3.6.2 Layer Adhesion

Good adhesion between the deposited layers plays a major role in the FDM process. When the semi-solid filament material is extruded from the nozzle it is pressed against the previous layer built as illustrated in figure 3.8a.Due to the high temperature and pressure which re-melts the surface of the previous layer to a new layer and enables them to bond with each other. The bond strength between different layers is lower than that of the base strength of the material. This means the strength of the FDM part is relatively lower in Z-axis than compared to XY-plane. For this reason, it is important to consider part orientation during the designing phase for part produced by the FDM process. Moreover, since the molten material is pressed against the previous layer, its shape is deformed to an oval. This implies that FDM parts will always have a wavy surface, even for low layer height, and that small features in the part produced may need to be post-processed after printing[19].
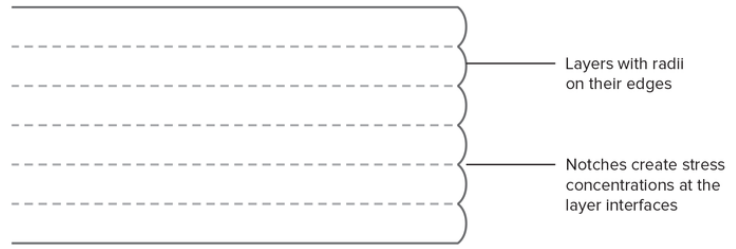
Figure 3.8: Schematic (b) and actual (a) representation of the FDM constructed layer by layer [19]

3.6.3 Effect on Printing Path Width

Now considering the adjacent paths illustrated in figure 3.9, it is constituted by a range of scenarios:(i) adjacent path very close to each other which end up in an overlap of the path and excess deposition of filament (ii) adjacent path distance from each other which results in gaps and minimal or no bonding between them which decreases the structural integrity of the part being produced. Thus optimizing the width of the path becomes necessary. This can be done by extruding more or less material by changing the feed rate. Despite the fact that the thicker path leads to better bonding and thus better mechanical performance, it will fail to meet the geometrical resolution.
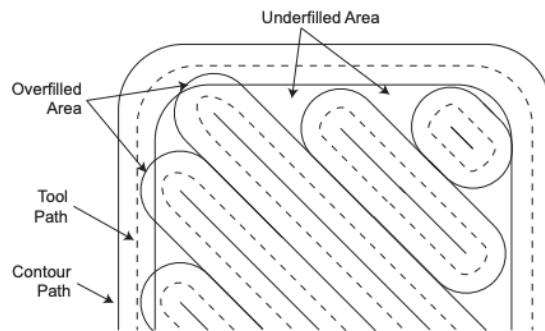
Figure 3.9: Schematic illustration of the path influence

4 DEBINDING AND SINTERING

4.1 Thermogravimetric Analysis Process

Thermogravimetric analysis (TG) measures the change in mass of a test specimen as a function of time. The actions causing the mass change can be an example of reduction, absorption, oxidation, vaporization and decomposition. This method is generally used to examine the thermal stability of the material in various conditions and also used to investigate the kinetics of the physicochemical process occurring in the test specimen. The mass change characteristics are based on experimental conditions like specimen mass, shape, nature of the sample holder used, nature of the atmosphere in the chamber etc. The TG curve is usually plotted with the mass change in terms of percentage and temperature or time in the first and the second co-ordinates respectively.[14]
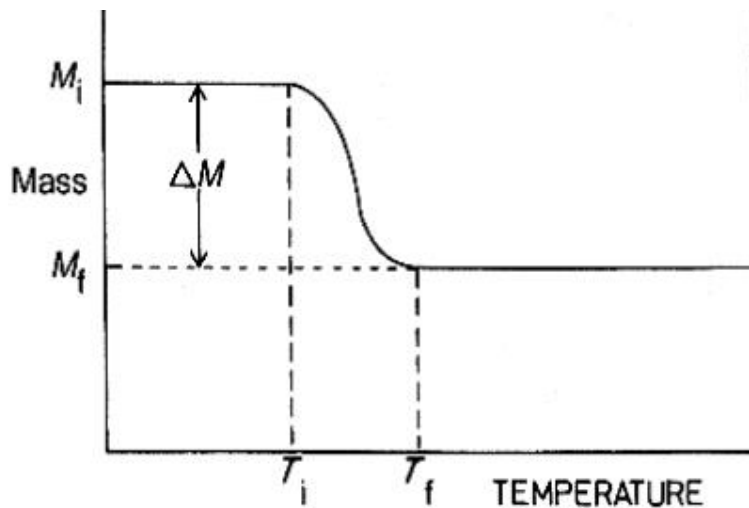
Figure 4.1: Schematic representation of a TG curve
[9]

With the definition of the optimal parameters required for printing the test specimen were subjected to a thermogravimetric process, by carefully considering various parameters and the kind of atmosphere required.

4.2 Debinding Process

Debinding is the process which explains the binder material removal from the green body. As a result of this at the end of the debinding process, the part produced will contain pure metal in it. The debinding process is perhaps the most crucial part of this experiment. The achievement of a good result depends on how carefully and precisely the binder is removed. Thermal debinding involves the removal of the binder from the sample at a marginally elevated temperature by heating the sample with a controlled rate at different atmospheric conditions. In thermal debinding, the molten binder material flows to the surface faster than it evaporates, this explains that the debinding rate depends on the heat put in for degradation.

4.3 Sintering Process

Sintering is a thermal treatment that makes the particles bond together by subjecting the pre debinded part to a high temperature. By doing so bonds between the metal particles will start to structure. In this process, the particles combine tighter and tighter by eliminating the pores created. As the temperature increases at some point, most of the pores will be eliminated and form a more dense body. As a result of this, the sample will undergo a rapid shrinkage. One most important aspect of sintering is that even though the temperature during sintering is very high they never cross the melting temperature of the material considered. The maximum sintering temperature is a bit below the melting temperature of the material. Sintering is primarily a thermal treatment method used for densification.

4.4 Binder

The secondary component that makes up to the metal filament is the binder. While the metal powder, in this case, stainless steel 316L provides the structural properties to the finished part. The binder material won't contribute to the properties since it won't be present at the end. The binder material plays a very vital role and the benefit of metal-infused filament process depends on the performance of the binder.

In this study using the virtual foundry filament, it was examined from the TG run that the binder material consists of a combination of different components: a polymer and a filler material. The proportion of the polymer and filler in the binder is unknown. The polymer material used in this filament was PLA which was confirmed from the FTIR run explained in the following section and the filler material is some type of wax material.

The molecular weight and the chemical structure helps the polymer and filler material from not completely mixing. A difference in the melting point between these materials promotes the selective removal of separate components during the post-processing process.

Waxes favour melting at low temperature (<100°C) while polymer tends to melt at a higher temperature(>100°C). This suggests that the wax is the first major component to be removed which happens during the debinding[4].

4.4.1 Secondary Binder

The main function of the secondary binder is to provide the structural strength to the printed green part before debinding and sintering. Cause of its structural benefits during the printing process the secondary binder component is referred to as backbone. The secondary binder is usually made up of polymer.

Its this backbone polymer which has the highest melting temperature when compared to the other components in the binder.The removal of the backbone polymer is the most critical and time-consuming part.Polylactide or Polyethylene is the most commonly used binder polymers since they provide the necessary structural strength. They have a low melting point and low viscosity which constitutes efficient printing[4].

4.4.2 Primary Binder

The primary binder is commonly a wax or a wax-like material. The main purpose of the primary binder is to provide flexibility and moldability while being easy to remove. Waxes have a low melting point and reduce easier than polymer, this allows them to be removed separately during the debinding process. Due to the low molecular weight of these wax components, the debinding process needs to be structured carefully to evaporate them easily while still keeping the shape of the printed part intact. The most commonly used fillers are paraffin and bee wax[4].

4.5   Fourier-Transform Infrared Spectroscopy (FTIR)

Fourier-transformation infrared spectroscopy is a technique adopted to determine the infrared spectrum absorbed or emission from the sample. This process was conducted to measure what material absorbs light at specific wavelength[14]. An FTIR test was conducted on a small piece of Commercially available PLA as a reference and later a second test on the virtual foundry stainless steel 316L filament to investigate the presence of any PLA material in the filament. The curve is shown in figure 4.2 confirms the presence of PLA in the stainless steel 316L filament as it follows the same spectral wavelength curve as that of the general PLA material.
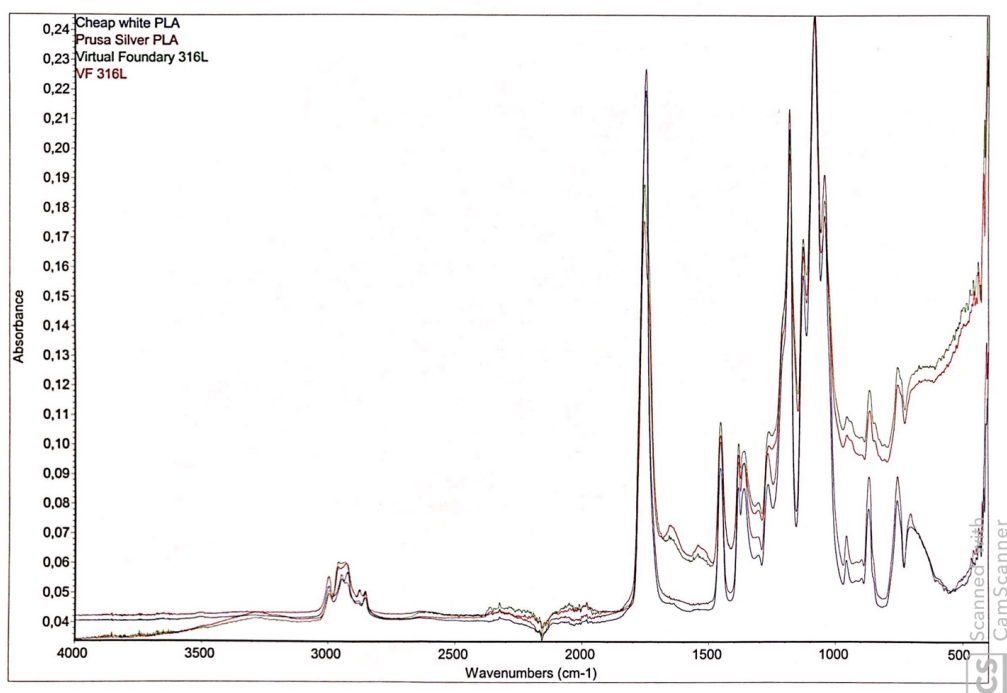
Figure 4.2: Illustration of the FTIR curve

5 EXPERIMENTAL TECHNIQUE- PRINTING

5.1 Experimental Work

In this chapter, the material used, equipment and condition used in the manufacturing of the test specimen are described in detail.

5.1.1 Material and Filament

As given in the aim the metal infused filaments and their properties for their use in the 3D printer are explained below. Table 5.1 gives data on the properties and printing parameters for the two materials used. The materials used in this study were the two commercially available metal filaments in the market: steelfill from colorfabb with 30% in weight of Stainless steel and stainless steel316L filament from virtual foundry with 83% in weight of metal as shown in figure 5.1a and 5.1b respectively. The two grade were supplied in filament form of about 1.75mm diameter, as desired by the FDM printer used in this study. Several extrusion trials were performed in various conditions to study the desired output. The filament with 30% in weight from colorfabb was initially used to calibrated the 3d printer and also to test the nozzle for any abrasion. Based on the high density among the two different set of filament , virtual foundry SS316L filaments with 83%metal density was selected for later study and experiments.

| (a) | (b) |
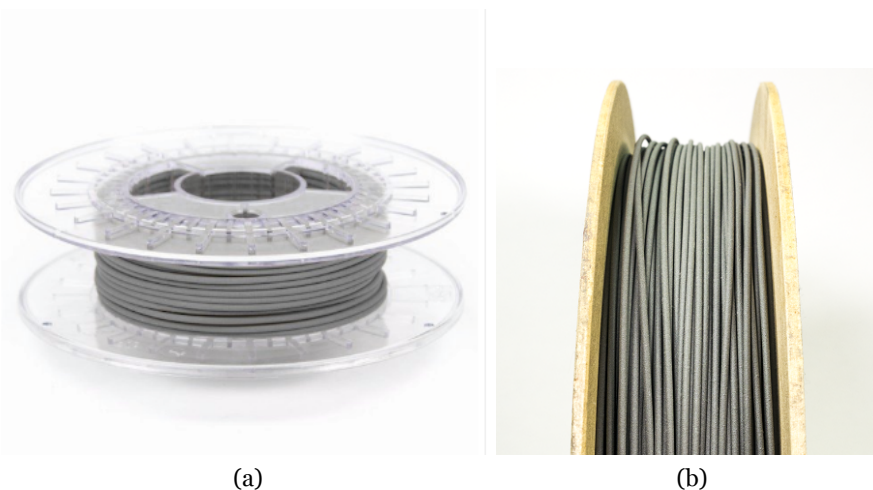
Figure 5.1: ColourFabb (a) and virtual foundry stainless steel 316L (b) filaments [15][18]

Table 5.1: Data on the properties and priniting parameters for the two materials used :Steelfill from Colorfabb and SS316L from Virtual foundry

PROPERTY	MIN	MAX	AVG	UNIT
Steelfill from ColorFabb				
Density	—	3.13	3.13	g/cm3
Extrusion Temperature	190	210	200	°C
Diameter	—	1.75	1.75	mm
Percentage by mass	—	30	30	%
Printing speed	40	80	60	mm/s
Stainless Steel 316L filament from Virtual Foundry				
Density	—	3.5	3.13	g/cm3
Extrusion Temperature	210	235	222	°C
Diameter	—	1.75	1.75	mm
Percentage by mass	—	83.5	83.5	%
Printing speed	40	80	60	mm/s

5.1.2 Printer and Nozzle

The Virtual foundry filament is a metal-polymer composite filament which enables its application in any Bowden style or direct drive extrusion printers. The equipment used for printing the virtual foundry filament is a Prusa MK3 i3 FDM based printer as shown in figure5.2.This is usually used to print plastic-based filaments such as PLA(Polylactic acid), ABS(Acrylonitrile butadiene styrene) etc.The filament with at least 83% of metal and a diameter of 1.75mm is acquired from Virtual foundry in this study . The placement of the filament is carefully examined to make sure there is no breakage of the filament during the printing process. Also a rectangular printing pattern was chosen based on the explanation illustrated in section 3.6.1.The varied parameters in the study were the extrusion temperature,layer height, printing speed which is represented in table.

Figure 5.2: Prusa mk3 i3 printer
[8]

A final set of customized printing parameters (layer height 0.1mm, printing speed 50mm/s, extruder temperature 201◦C) was carefully iterated and developed for this study and used to print a green part as shown in table 5.2. These parameters were developed based on the visual observation of the output in the test specimen. However, due to the higher working temperature and density of the metal-infused filaments compared to thermoplastics, a special ruby nozzle shown in figure 5.3 had to be used to produce a stable flow of the filament, thus assuring high-quality print outputs. Due to the use of high density filament the use of ruby nozzle proved effective.

Figure 5.3: Olsson Ruby Nozzle
[7]

An even distribution of glue and ethanol on the bedplate ensured a good adhesion of the filament to the base thus reducing the wrapping or distortion.

In this work, a cube of 10*10*10 mm as illustrated in figure 5.4 below was printed as a test specimen. These cubes were printed at both 210◦C and 235◦C .Fourier-transform infrared spectroscopy was carried out to examine the PLA presence in the filament. The 3D printed cubes were subjected to a series of iteration through the debinding and sintering process which is being explained in the next chapter.

Figure 5.4: Specimen Cube used for all test analysis in this thesis

5.1.3 Printing Parameters

Several test runs were first performed to determine the printing parameters of the green body using the Prusa 3d printer and printed by virtual foundry stainless steel 316L filament. These are outlined and broken down into concepts as illustrated in table 5.2.

In addition to the above mentioned operating parameters, few other details regarding the print surface on the bed were evaluated during this process and are mentioned as follows. The Stainless steel 316L filament showed low adhesion to the surface of the print bed.

The solution found out for this problem was the use of glue and ethyl alcohol by evenly spreading it on the surface of the print bed. This ensures good adhesion of the filament with the printing bed.

Table 5.2: Pugh Matrix

CONCEPT CRITERIA	CONCEPT A	CONCEPT B	CONCEPT C	CONCEPT D	CONCEPT E
Layer Thickness	0.2	0.3	0.35	0.1	0.1
	-	-	-	+	+
Extrusion Width	0.4	0.6	0.6	0.6	0.6
	-	+	+	+	+
Infill Density	10%	50%	100%	100%	100%
	+	-	+	+	+
Infill Orientation	90°	90°	90°	90°	90°
	+	+	+	+	+
Infill Pattern	Gyroid	Rectilinear	Rectilinear	Rectilinear	Rectilinear
	-	+	+	+	+
Printing Speed	70mm/s	60mm/s	55mm/s	50mm/s	50mm/s
	-	-	+	+	+
Extruder Temperature	195°C	215°C	230°C	210°C	235°C
	-	+	-	+	+
Build Plate Temperature	60°C	50°C	40°C	55°C	55°C
	-	+	-	+	+
Cooling Power	70%	80%	100%	100%	100%
	-	-	+	+	+
Total	-5	1	3	9	9

5.2 Results and Discussion

In this section, the effect of printing condition, the printing parameters and the analysis of the test specimen (green body) is assessed.

Based on the visual observation and considering the printing parameters test specimen printed at 210°C showed better result than the test specimen printed at 235°C. Images of these test specimens printed at two different temperatures are in figure5.5 figure5.6 respectively.
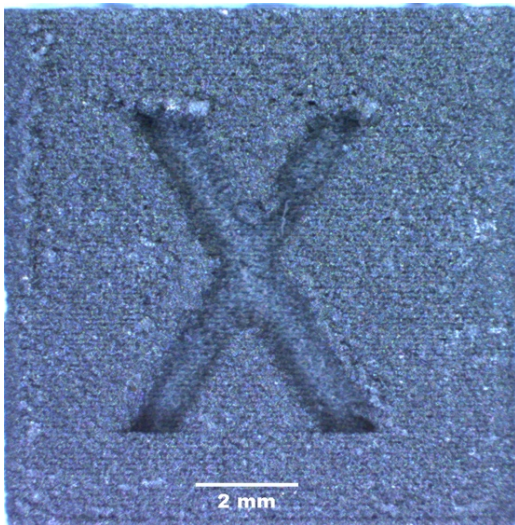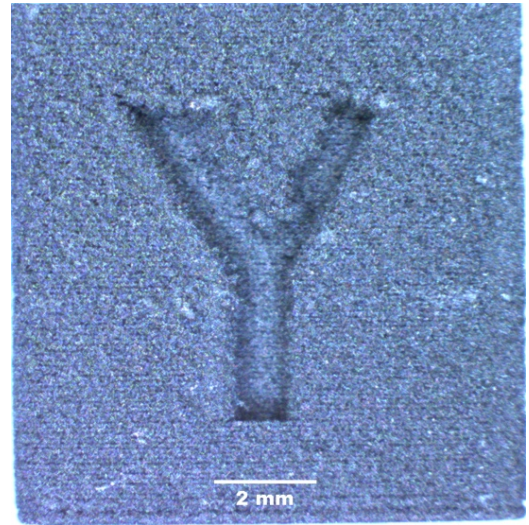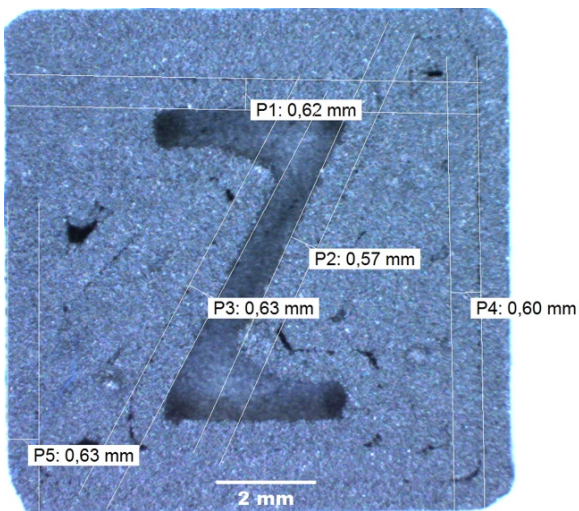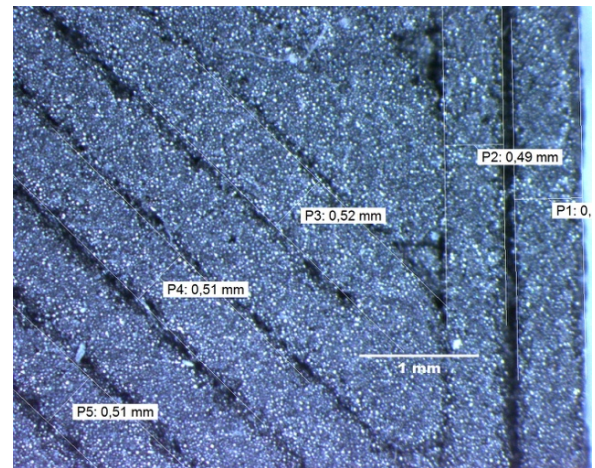
Figure 5.5: Microscopic (5x) images of green body test specimen printed at 210°C
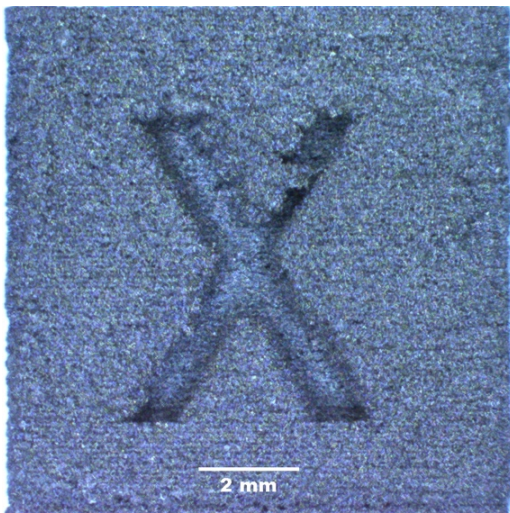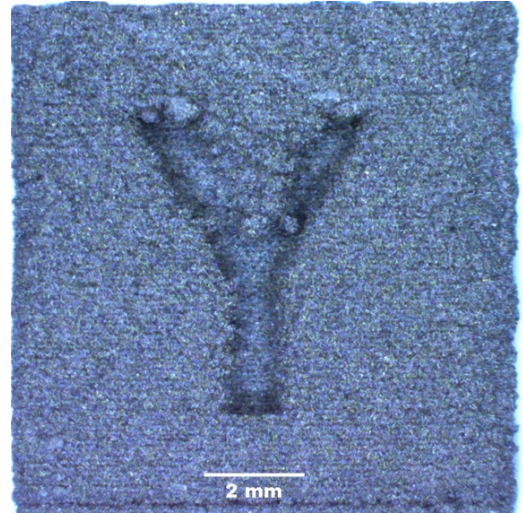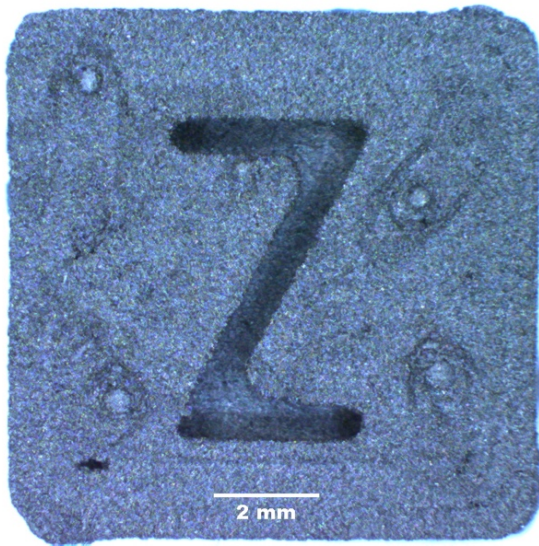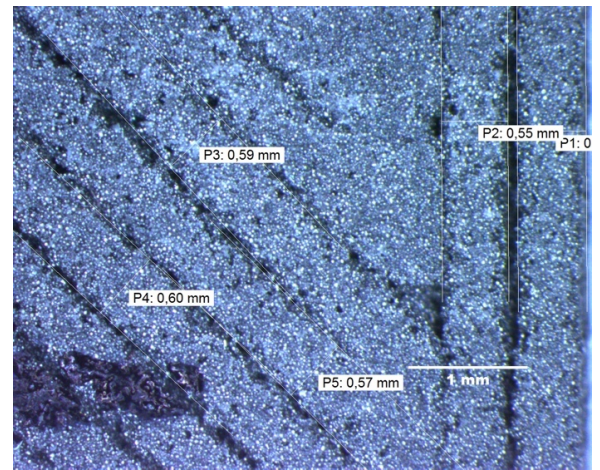
Figure 5.6: Microscopic (5x) images of green body test specimen printed at 235°C

These parameters were carefully studied and developed to achieve a good print. A good print is evaluated by yielding a thin strand that can be deposited in a destined location on the print area and adhering to the solidified earlier layer. Using the FDM process it is incapable of developing a complete dense body as the voids are coherently included in the printed part.

5.2.1 Green Body Analysis

The images illustrated in figure 5.7 a,bc, give a clear idea about how good the green body is printed using the Prusa 3D printer. The green body produced using the parameters discussed before was found to have a well-packed structure with no internal or external cracks. The green parts showed the same geometric resolution as per the dimensions used during the designing process. These green body specimens were evaluated based on visual and microscopic observations.

(a)

(b)

(c)
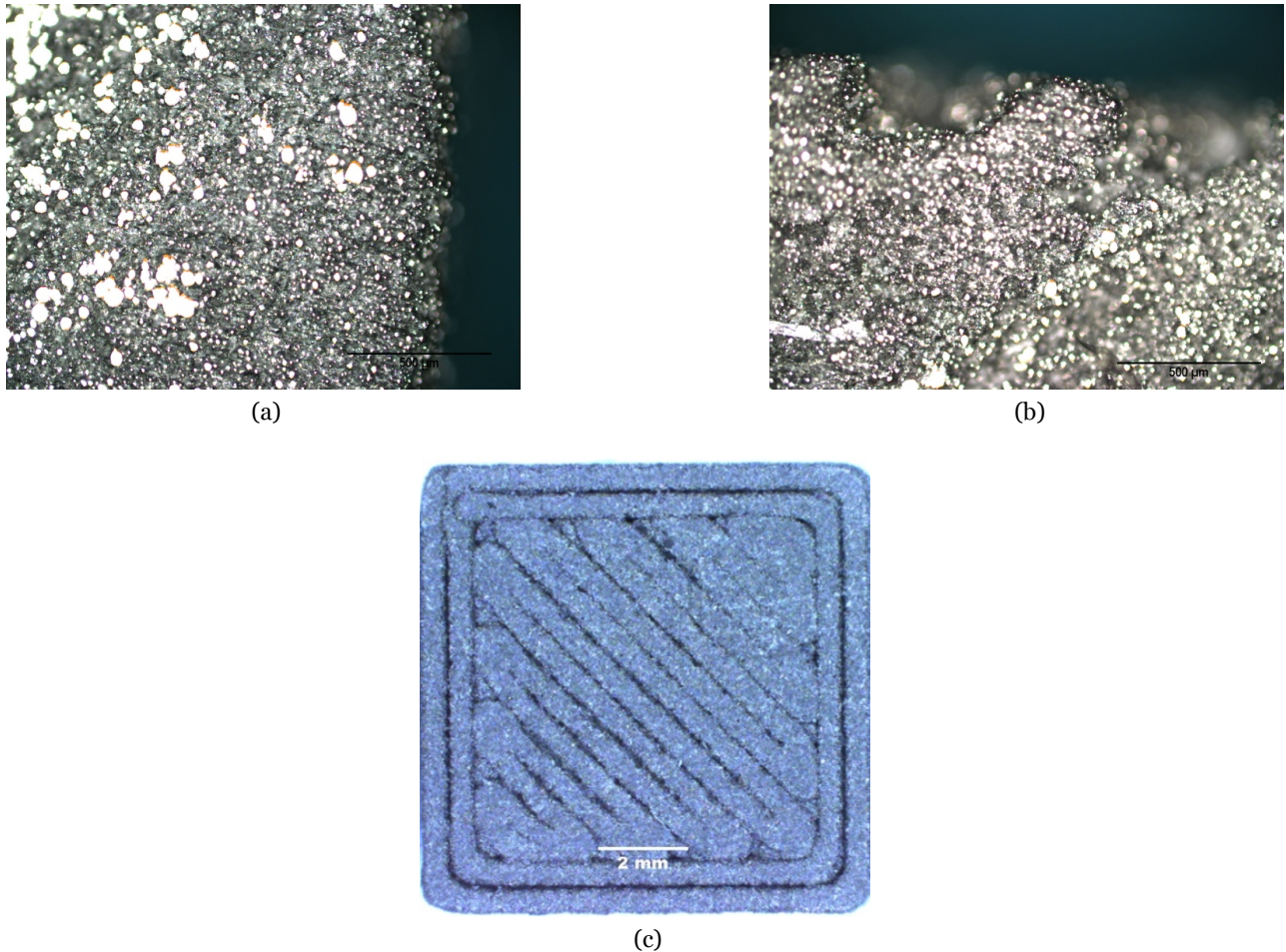
Figure 5.7: Microscopic view of the printed green body

This thesis work is an attempt to gather and establish a knowledge regarding filaments for metal 3D printing in an FDM machine. The tailored FDM process allows printing green body out of virtual foundry stainless steel 316L filament in a very easy manner .In the previous chapter, we have provided a deep outline of the FDM process and the parameters which govern them. This lead to the development of enabling effective and economical production of metal parts using the metal-infused filament through a commonly available FDM machine.

5.3 Conclusion

Based on the studies in this work the optimum parameters to achieve a rigid green body are shown below in table 5.3. The parameters listed are not comprehensive and may vary based on the appropriate hardware and software used but cover what we have found to be important and often adjusted parameters.

The main practical conclusion of this study was the results obtained with different printing parameters, the structural integrity which influences the mechanical property and geometric resolution. Another advantage of this developed FDM process is that the system allows for a straightforward change of material, as only a new filament has to be inserted into the print head, unlike the other AM techniques which are a time-consuming process.

Table 5.3: Optimal Processing parameters used

PARAMETER	DESCRIPTION	VALUE
Slicing		
Layer Thickness	Thickness of each layer of the printed FDM part	0.1mm
Extrusion Width	Width of the filament extruding from the nozzle.	0.6mm
Infill Density	Relative density from totally hollow (0) to totally solid object(100).	100%
Infill Orientation	Orientation of the infill pattern relative to x-axis of the 3D printer.	0-90°
Infill Pattern	Pattern in which the inner portion of the part is filled. Rectilinear is used in this study.	—
Support Density	The relative density of the support material from none(0) to solid(1).	0-1
Support Orientation	Support material orientation relative to the X-axis of the 3D printer.	0-90°
Printing		
Printing speed	Rate at which the extruder moves during deposition of the filament.	50mm/s
Extruder Temperature	Temperature of the extruder during deposition of the filament.	210°C
BuildPlate Temperature	Temperature of the build surface during deposition of the filament.	55°C
Cooling Power	Power applied by the cooling fan to solidify the extruded filament	100%
Extrusion Rate	Amount of filament fed into during the printing process.	90%

6 EXPERIMENTAL TECHNIQUE- INITIAL POST PROCESSING

6.1 Experimental Work

In this Section information about the binders, post-processing techniques like debinding and sintering of the test specimen are described in detail.

6.1.1 TG Experiment

A TG graph illustrated in figure 6.1 gives a detail description of the mass loss in the test specimen over varying temperature with a constant ramp rate of 5°C/min in a hydrogen atmosphere. It can be noticed from the graph that the initial mass loss of 0.08% occurs at 114.8°C and gradually starts to increase over the temperature range until 600°C.Clear notification of two different major mass losses 10.31% and 2.96% from the curve can also be observed which states to the two different polymer present in the filament used. The first major mass change of 10.31% occurs over the temperature range of 252°C to 277°C and the second major mass change of 2.96% over the temperature range 366.4°C to 386.1°C respectively. A total mass loss of 13.47% from the test specimen was observed during this process.
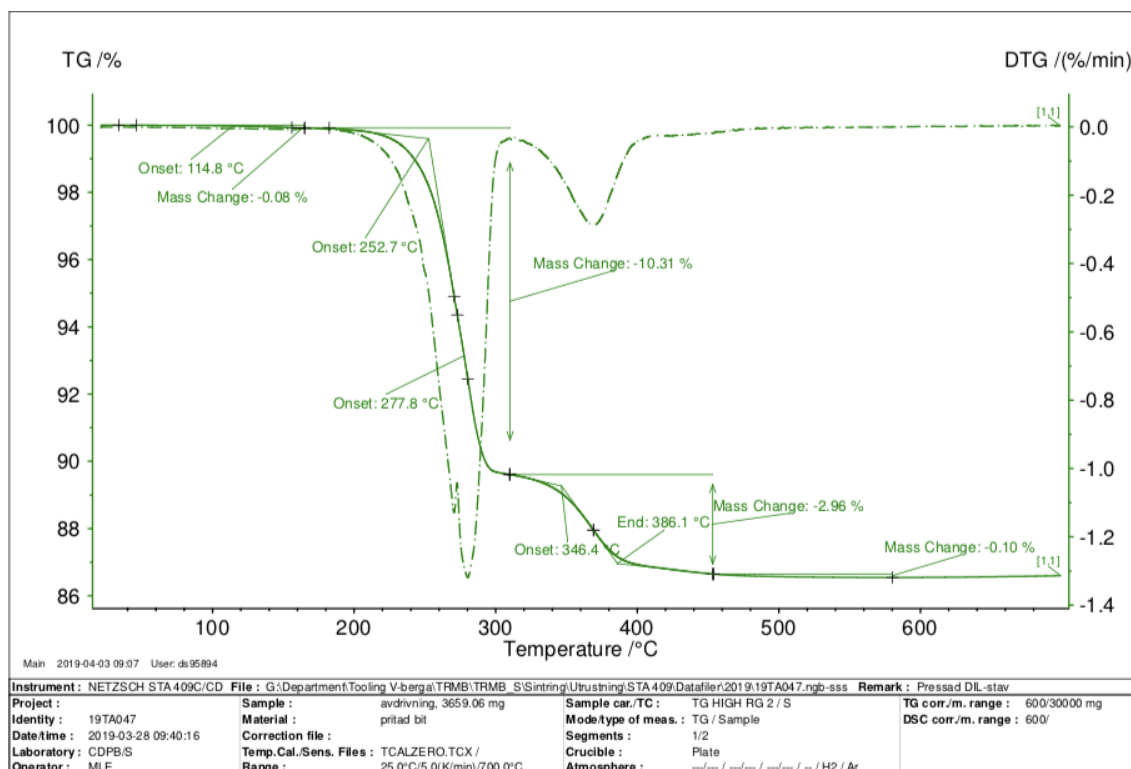
Figure 6.1: TG curve illustrating the mass loss of the test specimen in Hydrogen atmosphere

Using these inputs from the TG curve the debinding and sintering parameters were carefully constructed which are being explained in the next section. Also, a TG test runs on the sample was conducted in the synthetic atmosphere by keeping all other parameters same as they run with hydrogen. The mass loss and the curve are shown in figure 6.2.The mass loss after 450°C in both the test runs were approximately measured to be 13% but a difference in the shape after the TG run in both the cases were different. The test run with synthetic air showed more distortion in the test specimen when compared to hydrogen.
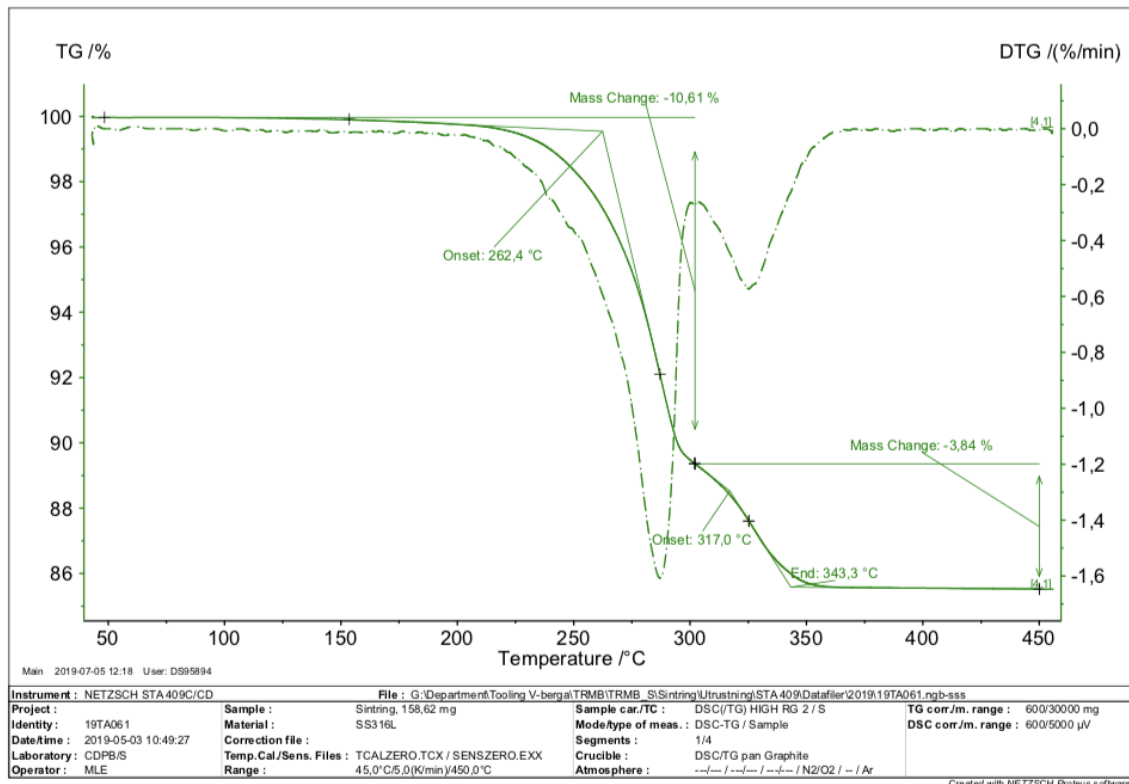
Figure 6.2: TG curve illustrating the mass change of the test specimen in Synthetic atmosphere

Also, a test runs on the specimen was conducted by placing the specimen in a graphite crucible and in contact with graphite powder to estimate the maximum temperature the sample withstands before melting. The curve representing the experiment on the test specimen with graphite is shown in the appendix C.

6.2 Debinding

In this experiment, the debinding process consists of two-stage: primary and secondary stage. The main objective of the primary debinding stage is to remove the surfactants and the main binder in the sample. The secondary debinding stage is used to get rid of the backbone binder and to start the sintering stage of the stainless steel component.

6.2.1 Another Debinding Method

One specimen which was printed at an operating temperature of 210°C and another specimen at 235°C.After these cubes were in the another debinding process for the specific given time and under specific pressure most of the primary binder (wax) was removed but the cubes were cracked after this process. It was also observed that one of the cubes printed at 210 °C was not subjected to cracking. This cube was later used for future study. Figure 6.3b illustrates the 4 different cubes printed at two different temperature that were subjected to the another debinding process.

Figure 6.3: Illustration of the sample cubes which were printed at 210°C (a) and 235°C (b) respectively

The exact reason for the formation of the cracks on the cubes were unknown since the temerature cycle during this process was not optimised for the type of binders present in this study.

6.2.2 Thermal Debinding Method

In order to understand the phase transformation and decomposition of the printed plastics a new test specimen was printed at 210°C and subjected to a thermal debinding process by carefully considering the parameters for the process. Melting points of the primary and the backbone binder were assessed from the curve as shown in figure 6.4.From the curve, the glass transition of the backbone binder was observed at 82°C which related to the glass transition temperature of PLA.
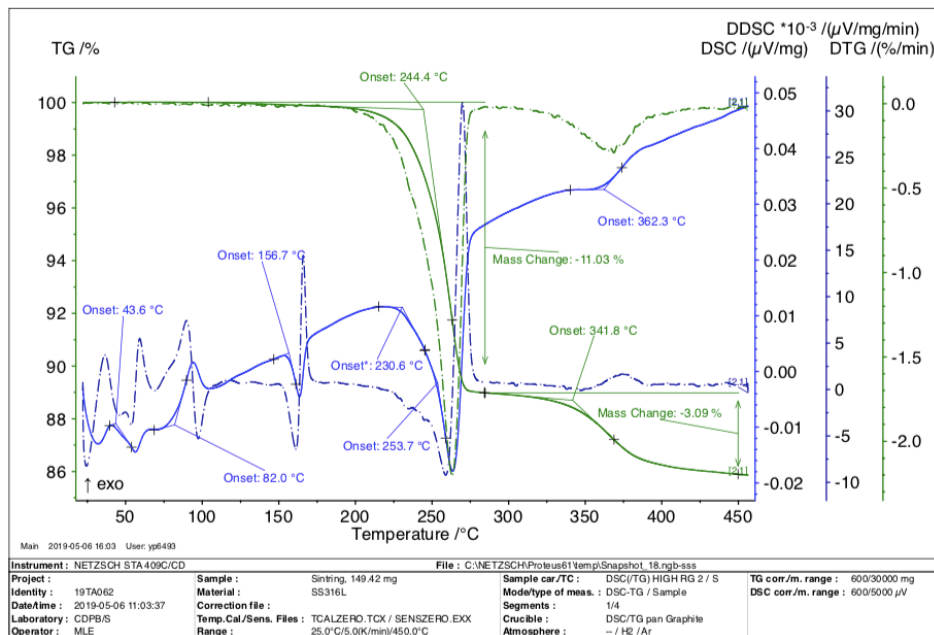
Figure 6.4: Curve illustrating the mass loss and melting points of the binders

Gathering the important data from the curve mentioned above the extracted cubes which were printed at 210°C were now considered for a thermal debinding test run. One part of the cracked cubes was subjected to a thermal debinding process with a ramp rate of 5 k/min in hydrogen atmosphere up to 450°C. The curve relating to the test run is illustrated in figure 6.5.A comparison of the sample piece before and after thermal debinding is explained in the result section.
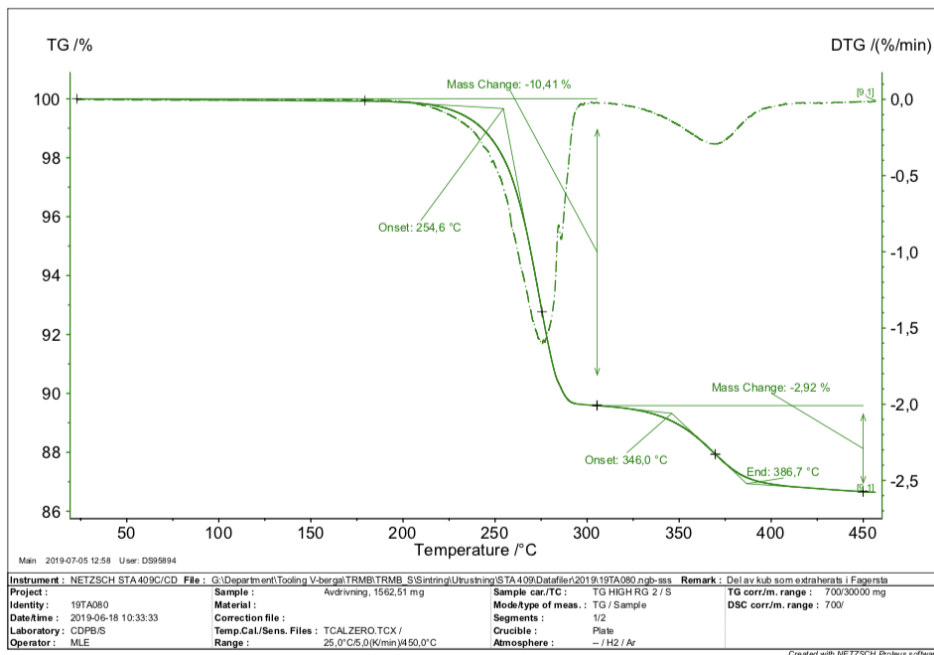
Figure 6.5: Curve illustrating a thermal debinding stage of the test specimen after it has undergone initial debinding stage

An additional experiment with a combination of thermal debinding and sintering process was carried out on a newly printed test specimen in Elink sintering furnace using the parameters used for binder jet post-processing. These parameters were not optimised for the binders present in the test specimen. This experiment is given in appendix D.

6.3 Sintering

In this work the final debinded test specimen pieces were later subjected to an sintering process with a ramp rate of 5 k/min up to 1100 °C in an argon atmosphere. The gas flow during the sintering cycle was maintained stationary to reduce the effect of carbon deposition on the test specimen. Along with that few titanium pieces were statically placed in the furnace as shown in the figure 6.6 to absorb the carbon molecule. The curve for the sintering process is illustrated in figure6.7a and 6.7b.

Figure 6.6: Illustration of titanium pieces placed in the TG machine

The curves (a) illustrated below gives an overview of the sintering process from start to end and the change in mass in the test specimen is being represented by the green curve and the temperature by the red curve respectively.

There was a tendency of mass gain at high temperature (b) due to pick up of carbon from the polymer residues present inside the Aluminium tube. But this needs to be further investigated.The images of the test specimen after the sintering process is represented in figure 6.8.
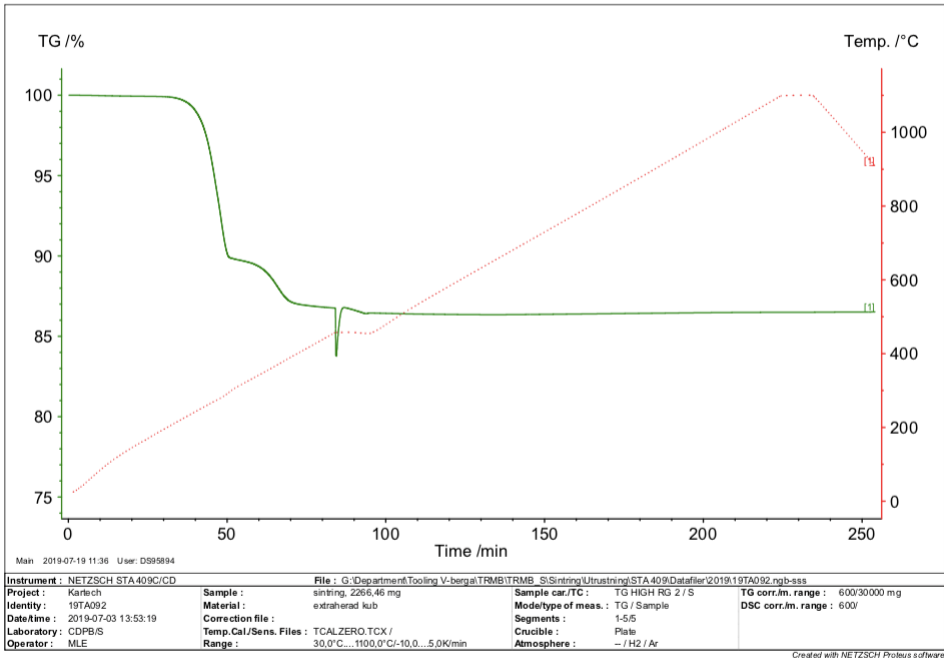
(a)
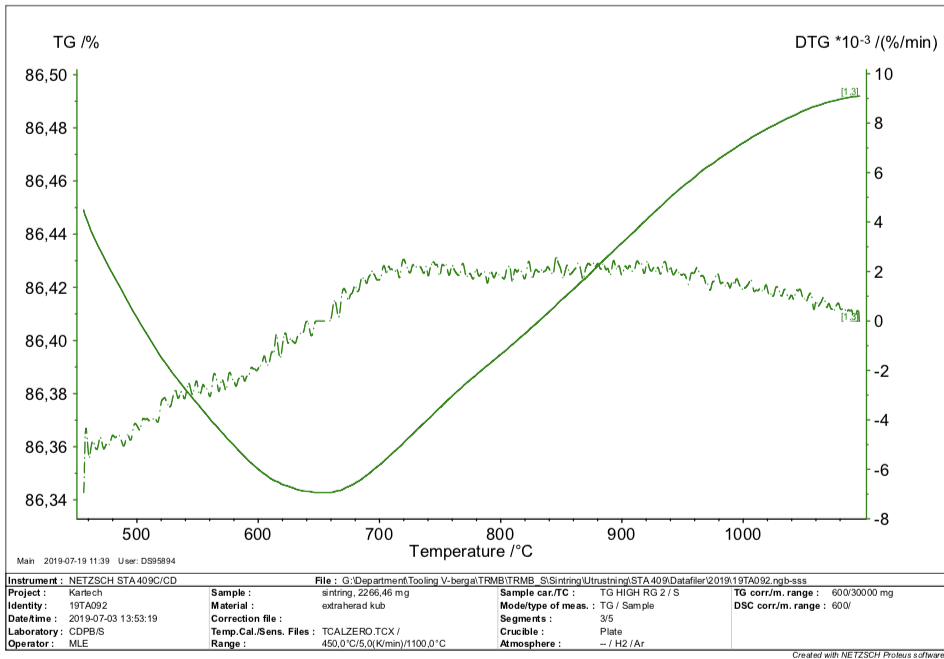
(b)

Figure 6.7: Illustrating the sintering curves of the completely debinded test specimen
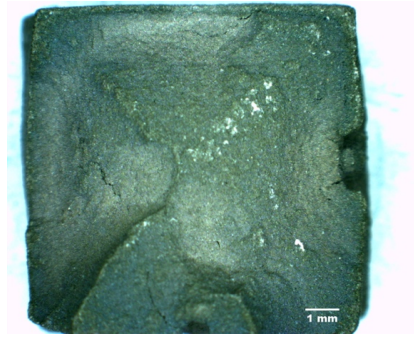
Figure 6.8: The Sintered test specimen

From figure 6.8 it can be identified that the formation of carbon deposition on the test specimen leads to the less metallic finish output. Carefully Controlling the gas flow during the sintering process and also in improving the surface properties of the specimen can result in a better outcome. A combination of debinding and sintering was carried out in an industrial graphite sintering furnace in a vacuum atmosphere. The curve and the process parameters used in this test run are illustrated in appendix E.

6.4   Results and Discussions

In this section, the effect of debinding, sintering and comparison between the test specimen is assessed.

6.4.1   Debinding Defects

The fundamental cause of thermal debinding defects is due to rapid heating. A very slow and steady heating process is needed to avoid defects. In thermal debinding process, the binder component is degraded into gases. If these gases formed in the specimen is big and if there are no proper pore channels created inside the specimen then pressure builds up inside the specimen creating stress. This pressure build-up can lead to cracks and distortion which can be seen in the figure below. The debinded part (to the left) is compared to the actual printed green body (to the right) in the figure 6.9a and the distortion phenomenon in the debinded specimen is visible. Thus by decreasing the heating rate the gas developed inside the sample won't be rapid and this effect can be reduced. Also by employing appropriate support for the specimen during thermal debinding can reduce the amount of distortion caused. Good airflow around the specimen ensures that the formed gases are removed quickly thereby reducing the pressure inside.
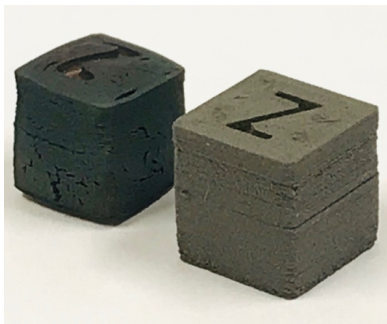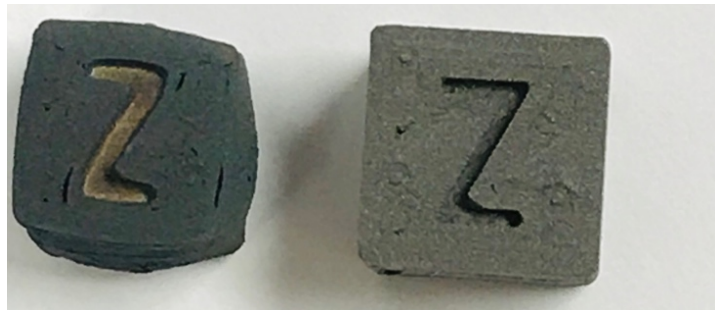
(a)   (b)

Figure 6.9: Comparison between debinded (left) and actual printed (right) test specimen

The main defects that occur during debinding are caused due to the stress involved in the sample. Apart from the effects of Gravity and loss of binder material that makes the sample exposed to defects during debinding, the binder extraction itself causes stress inside the sample which can be seen in figure 6.10 . A CT scan of the debinded sample gives a good analysis of the entrapped gasses evolved from the burning of the binder during the debinding process.

This lead to the most common debinding defects such as distortion and cracking. Hence at most care needs to be taken in the removal of these binder materials by still keeping the shape of the green body intact. Different debinding methods such as thermal and solvent
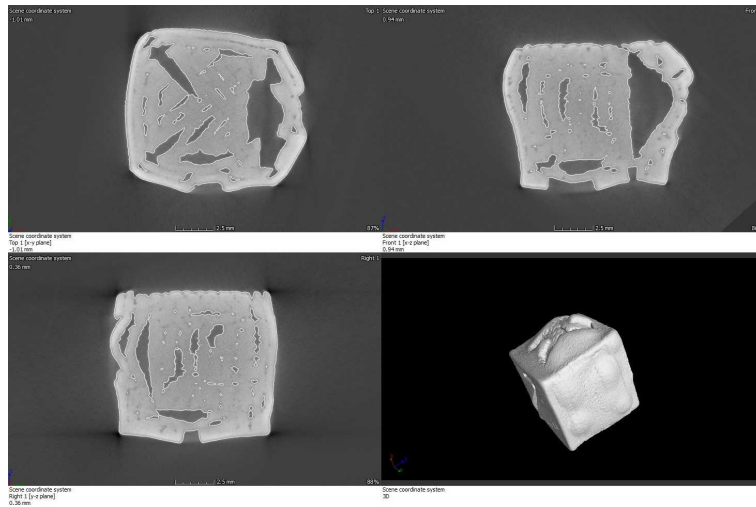
Figure 6.10: Computed tomography scan of the test specimen

cause different defects. For a better result, a common practice is to employ both solvent and thermal debinding in the form of a two-stage debinding process. Cause of the two-stage debinding, problems for both this process is encountered. Some defects will also be rooted in the previous printing stage.

6.4.2 Sintering Defects

The sintering is the last step in the post-processing stage. It is in this process that the sample gets its final strength and the desired result are shown. It is in this process where the damages from the previous stages will be revealed. The main principle during sintering is based on densification and shrinkage. Correspondingly the most common sintering defects will also be related to dimensional control. Another common cause of sintering defects is the atmosphere.

For a rewarding result, atmosphere control is essential. In addition to the atmosphere and dimensional defects the other recognizable defects: cracking, distortion and blisters are all common sintering processes. Few of them are discussed below.

- Low density: If the density after sintering is not as large as desired, altering the heating rate can lead to the densification of the sample piece. The max temperature can also be increased below the melting point of the metal to increase the density or altering the length of the max temperature time. Figure 6.11 illustrates the test specimen with a larger number of pores, thus implying to the low dense structure found.
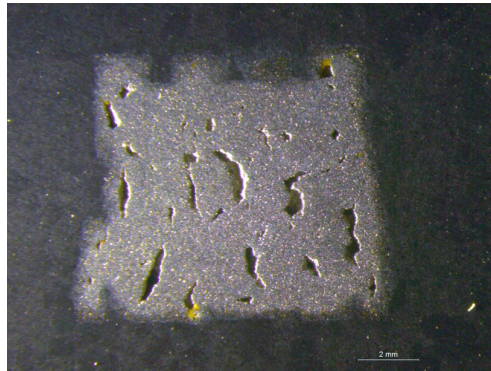
Figure 6.11: Cross-sectioned microscopic view of the test specimen

- Low properties: Low porosity mainly refers to poor mechanical strength. This could be a cause of incomplete densification. Increasing the sintering temperature could reduce the risk of low porous structure but too intensive heating results in poor properties due to grain growth. Hence the sintering cycle should be carefully monitored and controlled to achieve a promising strong result.Figure 6.12 illustrates the largely deformed test specimen due to rapid heating.

Figure 6.12: Illustration of the deformed test specimen

- Cracking: The most typical cause for cracking is due to rapid heating during both debinding and sintering cycles. Therefore by reducing the heating rate at the initial stages of sintering, it will allow the sample to build up strength before they get exposed to higher stress.
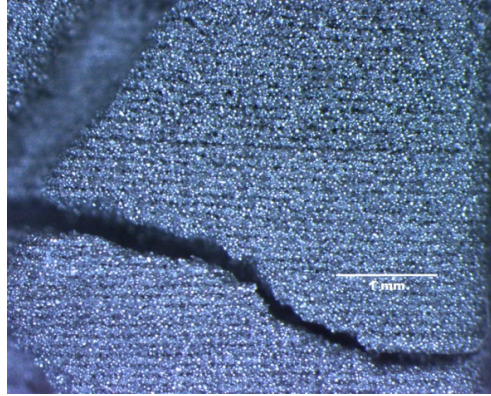
Figure 6.13: Microscopic view of the Crack formed on the test specimen

6.5 Summary

The figures illustrated below gives a comprehensive picture of the experiment performed in this thesis work, enabling a direct comparison of the specimen parts and a clear idea of the relative importance of the various parameters.

It can be observed from the figure 6.14a that the printing lines on the bottom surface of the test specimen resulted from the FDM process can be noticeable. These printing lines do not vanish during the sintering process, leading to a high roughness with a normal appearance. An analysis was done to investigate these lines on the sintered part, it can be observed that in some areas of the printed part the printing lines have no contact to each other, thus leading to a regular open porosity. In the case of printing a multilayer sample, these printing gaps are then filled by material from the next layer in the z-direction, thus resulting in a low porous structure in the core. This can result in a pore-free and fine grain microstructure can be achieved.
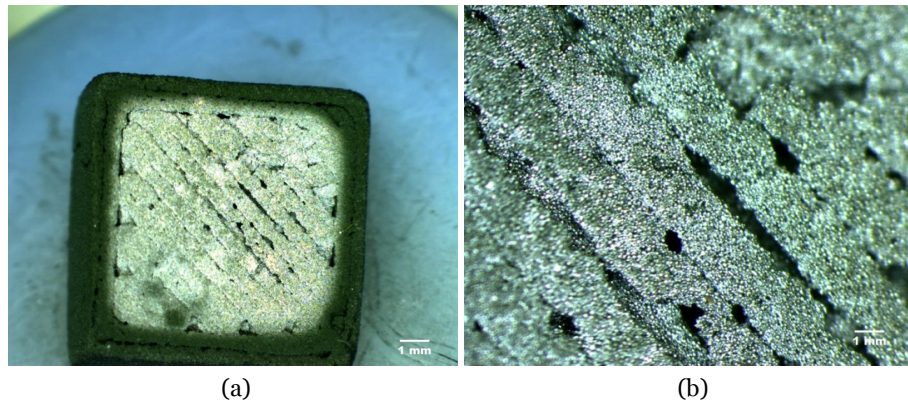
Figure 6.14: Sintered test specimen with visible printing lines
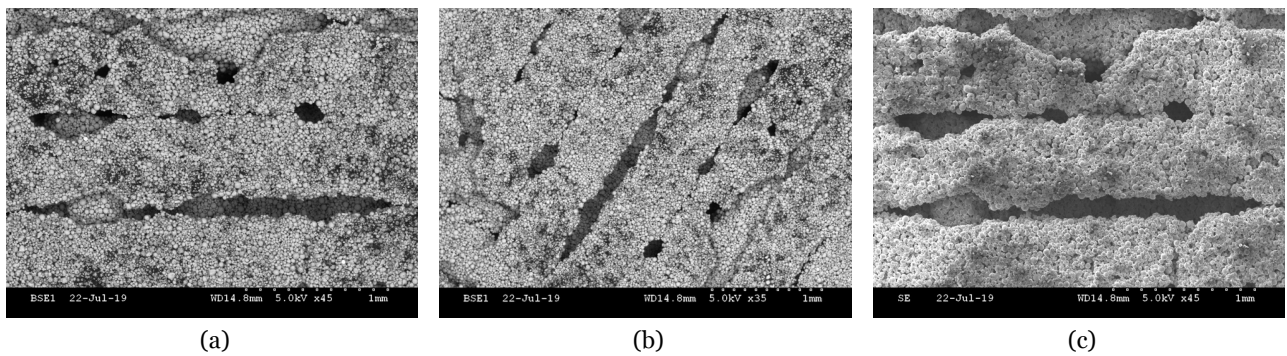
Figure 6.15: Magnification of the visible printing lines

A comparison between the test specimen before and after thermal debinding is illustrated below in figure 6.16b which explains the shrinkage factor. Figure 6.16a shows the parts after it undergoes the first stage of debinding and figure 6.16b shows the sample part which was subjected to a thermal debinding as explained in the previous section. Clear notification of healing of cracks can be observed cause of the shrinkage phenomenon.
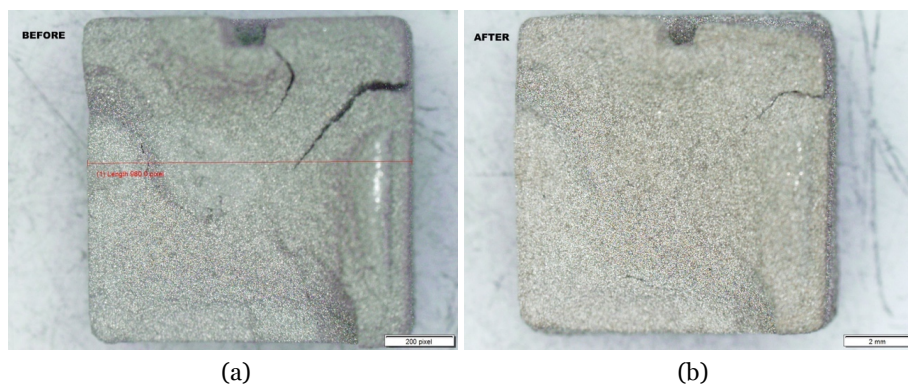
Figure 6.16: Illustrating the shrinkage of the test specimen during the debinding stages

A comparison of the test specimen after the debinding stage and after the sintering stage are

illustrated below in figures 6.17a and 6.17b. The healing of cracked formed in the specimen can be noticed after the completion of the sintering process and also the metal grains on the surface of the specimen seems to have bonded to each other rigidly.

(a) (b)
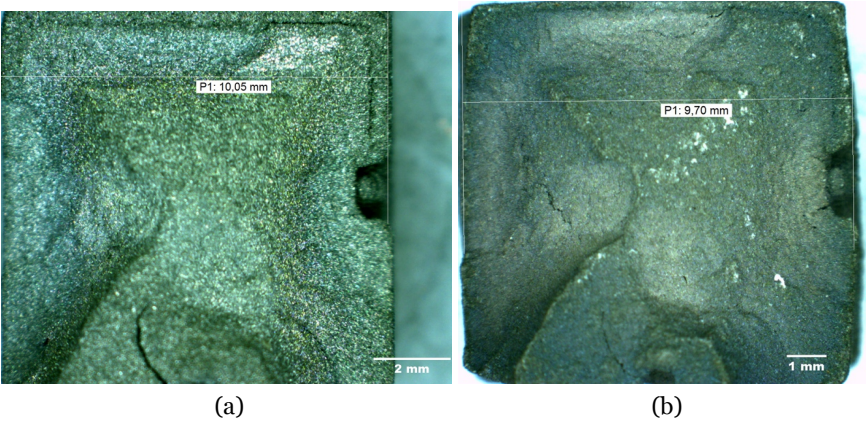
Figure 6.17: Illustration of the test specimen after debinding stage (a) and after sintering stage (b)

Additional microscopic images of the specimen are illustrated in figure 6.18.

(a)

(b)

(c)

(d)
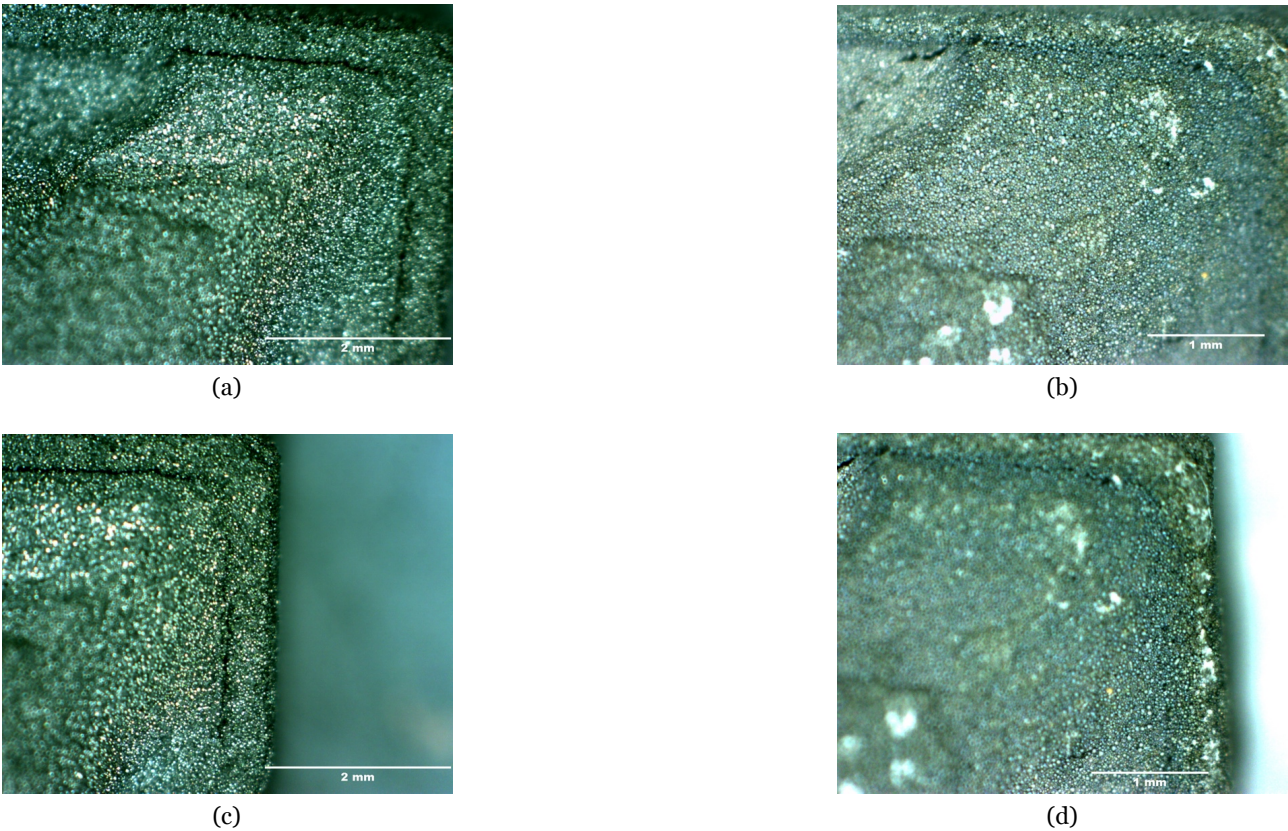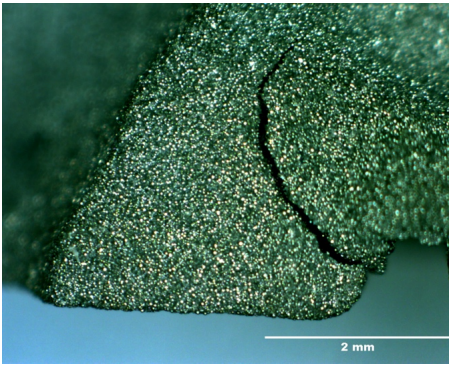
(a)
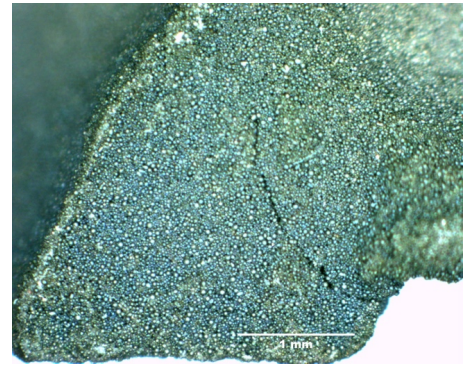
(b)

Figure 6.18: Microscopic images of debinded vs sintered specimen

7 CONCLUSION

The described FDM process in this thesis work allows printing green part out of Virtual foundry stainless steel 316L filament in a straightforward way, however, the surface properties need to be after treated for surface critical based applications. Debinding and sintering of the sample was the most challenging part and to control all the parameters added up to the challenge. After a series of trials, a set of parameters and equipment were selected with minor parameter alterations if necessary. It was also found out that the shrinkage rate from the green part of the final metal part varied in x, y and z directions. Virtual foundry stainless steel 316L is an upcoming and encouraging way of producing metal Additive Manufacturing parts and there is always space for future investigation in this area of Additive Manufacturing. The optimal Printing parameters finalised in this master thesis is given below.

Table 7.1: Finalised Optimal Processing parameters

PARAMETER	DESCRIPTION	VALUE
Slicing		
Layer Thickness	Thickness of each layer of the printed FDM part	0.1mm
Extrusion Width	Width of the filament extruding from the nozzle.	0.6mm
Infill Density	Relative density from totally hollow (0) to totally solid object(100).	100%
Infill Orientation	Orientation of the infill pattern relative to x-axis of the 3D printer.	0-90°
Infill Pattern	Pattern in which the inner portion of the part is filled. Rectilinear is used in this study.	—
Support Density	The relative density of the support material from none(0) to solid(1).	0-1
Support Orientation	Support material orientation relative to the X-axis of the 3D printer.	0-90°
Printing		
Printing speed	Rate at which the extruder moves during deposition of the filament.	50mm/s
Extruder Temperature	Temperature of the extruder during deposition of the filament.	210°C
BuildPlate Temperature	Temperature of the build surface during deposition of the filament.	55°C
Cooling Power	Power applied by the cooling fan to solidify the extruded filament	100%
Extrusion Rate	Amount of filament fed into during the printing process.	90%

7.1 Future Work

As a conclusion, we believe there is always room for future improvement of the technique and also investigate on the printed samples for making this process more advantageous/competitive when compared to conventional ones for the production of a small batch of parts. Also more specific and use of different size nozzle diameter while printing the green body can be examined and researched. Also, a more in-depth look at the parameters used while printing the test specimen could be looked into further. The post-processing is what makes the green body into a complete metal body. The case of debinding and sintering to achieve a good mechanical property of the end product should be looked into and also a comparison of the AM technique discussed in this thesis project should be compared to other AM technique based on cost and time. A popular work would be to see if the metal-infused filament can be produced by metal injection moulding to accommodate them for printing in a commercially available FDM 3D printer. The FDM technique, therefore, has the potential to outpace the limitation related to the production of only prototypes and also on the mechanical properties of the produced part.

7.2 Final Words

References

[1]   Burkhardt, Carlo et al. "Fused filament fabrication (FFF) of 316L Green Parts for the MIM process". In: *European Congress and Exhibition on Powder Metallurgy. European PM Conference Proceedings*. The European Powder Metallurgy Association. 2016, pp. 1–7.

[2]   Carneiro, Olga S, Silva, AF, and Gomes, Rui. "Fused deposition modeling with polypropylene". In: *Materials & Design* 83 (2015), pp. 768–776.

[3]   Cooper, Kenneth. *Rapid prototyping technology: selection and application*. CRC press, 2001.

[4]   Engström, Sebastian. "Metal Injection Molding: A review of the MIM process and its optimization". In: (2017).

[5]   Gao, Wei et al. "The status, challenges, and future of additive manufacturing in engineering". In: *Computer-Aided Design* 69 (2015), pp. 65–89.

[6]   Gibson, Ian, Rosen, David W, Stucker, Brent, et al. *Additive manufacturing technologies*. Vol. 17. Springer, 2014.

[7]   INC, MatterHackers. *Olsson Ruby Nozzle Bundle*. 2019. URL: `https://www.matterhackers. com/store/l/olsson-ruby-nozzle-bundle-175mm/sk/MJ0GCUGT`.

[8]   INC, ORD Solutions. *Object Replication and Design,Original Prusa i3 MK3 - 3D printer KIT*. 2019. URL: `https://www.ordsolutions.com/original-prusa-i3-mk3-3d-printer-kit/`.

[9]   INC, Slideplayer.com. *Chapter 4 Other Techniques: Microscopy, Spectroscopy, Thermal Analysis*. 2019. URL: `https://slideplayer.com/slide/6458253/`.

[10] Kruth, Jean-Pierre. "Material incress manufacturing by rapid prototyping techniques". In: *CIRP annals* 40.2 (1991), pp. 603–614.

[11] LIMITED, SPI LASERS. *Additive Manufacturing Materials*. 2018. URL: `http://www. spilasers.com/%20application-additive-manufacturing/additive-manufacturing- materials/`.

[12] Manfredi, Diego et al. "Additive manufacturing of Al alloys and aluminium matrix composites (AMCs)". In: *Light metal alloys applications*. IntechOpen, 2014.

[13] Mutua, James et al. "Optimization of selective laser melting parameters and influence of post heat treatment on microstructure and mechanical properties of maraging steel". In: *Materials & Design* 139 (2018), pp. 486–497.

[14] Porter, Marie-Aude. *Effects of binder systems for metal injection moulding*. 2003.

[15] Solid, Printed. *Colorfabb Steelfill Filament*. 2018. URL: `https://www.printedsolid.com/ products/colorfabb-steelfill`.

[16]   Srinivasan, V and Bassan, J. "3D printing and the future of manufacturing". In: *CSC Leading Edge Forum*. 2012.

[17]   Steuben, John, Van Bossuyt, Douglas L, and Turner, Cameron. "Design for fused filament fabrication additive manufacturing". In: *ASME 2015 International Design Engineering Technical Conferences and Computers and Information in Engineering Conference*. American Society of Mechanical Engineers. 2015, V004T05A050–V004T05A050.

[18]   TheVirtualFoundry. *Stainless Steel 316L Filament*. 2019. URL: `https : / / shop . thevirtualfoundry.com/products/stainless-steel-316l`.

[19]   Varotsis, Alkaios Bournias. *Introduction to FDM 3D printing*. 2019. URL: `https : / / www . 3dhubs.com/knowledge-base/introduction-fdm-3d-printing`.

[20]   Weber, Christopher et al. "The role of the national science foundation in the origin and evolution of additive manufacturing in the United States". In: *Science & Technology Policy Institute* 1 (2013).

APPENDIX - CONTENTS

A   GANTT CHART
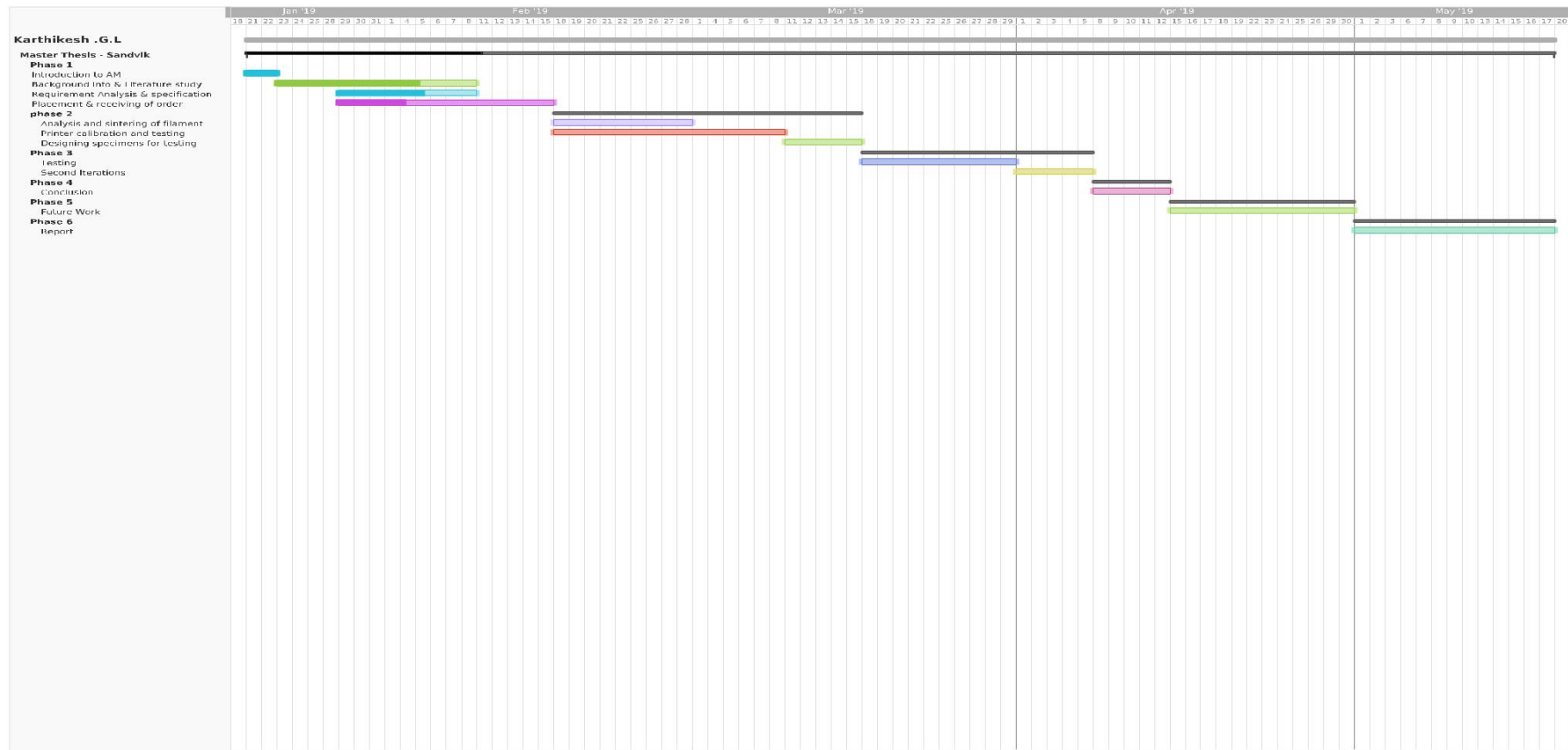
B   RISK ANALYSIS

Level 1	Level 2		Level 3
Risk	Probability	Consequence	Planned Action
3D Printer troubleshooting issues	High Probability	Cannot achieve a proper green body	Develop and use of calculated print settings and parameters
Shrinkage of brown body	Medium probability	Might result in collapsed final structure	To study and maintain proper sintering parameters

C   TG CURVES

DSC /(µV/mg)   DDSC /(µV/mg/min)

↑ exo

Onset: 1216.3 °C

[1,3]

[1,3]

Temperature /°C

1210   1215   1220   1225

Main 2019-04-05 13:47 User: ds95894

Instrument : NETZSCH STA 409C/...	File : G:\Department\Tooling V-berga\TRMB\TRMB_S\Sintring\Utrustning\STA 409\Datafil...\19TA052.ngb-sss	Remark : En liten printad bit som ligger i en grafitpulver...	
Project : 3D-Print	Sample : Smältpunkt, 37.45 mg	Sample car./TC : DSC/(TG) HIGH RG 2 / S	TG corr./m. range : 600/30000 mg
Identity : 19TA052	Material :	Mode/type of meas. : DSC-TG / Sample	DSC corr./m. range : 600/5000 µV
Date/time : 2019-04-05 09:56:48	Correction file :	Segments : 3/5	
Laboratory : CDPB/S	Temp.Cal./Sens. Files : TCALZERO.TCX / SENSZERO.EXX	Crucible : DSC/TG pan Graphite	
Operator : MLE	Range : 450.0°C/5.0(K/min)/1240.0°C	Atmosphere : -- / H2 / Ar	

Created with NETZSCH Proteus software

D   POST PROCESSING CYCLE

| DONE	1	2	3	4	5	6	7	8	9	
Segment Type / Segmenttyp (R / S)	R	S	R	S	R	R	S	R	R	
Temperature Setpoint / Temperatur börvärde (0-1650 grader C)	290	290	450	450	900	1100	1100	700	75	
Rate Or Time (Deg C / Min) / Hastighet eller tid (grader C /min)	3	30	3	60	6	3	240	4	15	
Guaranteed Flag / Garanterad flagga (J / N)	N	J	N	N	N	N	N	N	J	
Positive Deviation / Positiv avvikelse (0-1650 grader C)	0	40	0	5	0	50	50	0	0	
Negative Deviation / Negativ avvikelse (0-1650 grader C)	0	30	0	25	0	30	30	0	75	
Debind Event / Debind-händelse (J / N)	J	J	J	J	N	N	N	N	N	
Sinter Event / Sinter-händelse (J / N)	N	N	N	N	J	J	J	N	N	
Heaters On / Värmare på (J / N)	J	J	J	J	J	J	J	J	N	
Chamber Pressure / Kammartryck (0-1013 mBar)	400	400	400	400	400	400	400	400	400	
Hotzone H2 Gas Flow / Het zon H2-gasflöde (0-50 LPM)	5	5	5	5	5	5	5	0	0	
Retort H2 Gas Flow / Retort H2-gasflöde (0-50 LPM)	10	10	10	10	10	10	10	0	0	
Process Gas Select / Processgasval (N2 eller Ar)	AR	AR	AR	AR	AR	AR	AR	AR	AR	
Hotzone Process Gas Flow / Het zon processgasflöde (0-50 LPM)	0	0	0	0	0	0	0	5	5	
Retort Process Gas Flow / Retort processgasflöde (0-50 LPM)	0	0	0	0	0	0	0	5	5	
Cool Down Temperature / Nedkylningstemperatur (0-800 grader C)	0	0	0	0	0	0	0	700	700	
N2 Vent/Purge Event / N2-ventilation/urspolningshändelse (J / N)	N	N	N	N	N	N	N	J	J	

Program Name: / Programnamn: 316 FFF
Date: / Datum: 16.09.05
Time: / Tid: 09:50
Programmer: / Programmerare: PETER & MAGNUS
Comments: / Kommentarer:

E POST PROCESSING CYCLE AND CURVE

2019-05-02
2019-03-19 - 19SD009 - DMK80.2 - PRG40 - Master thesis, Vacuum process, 1200C, 180 minutes
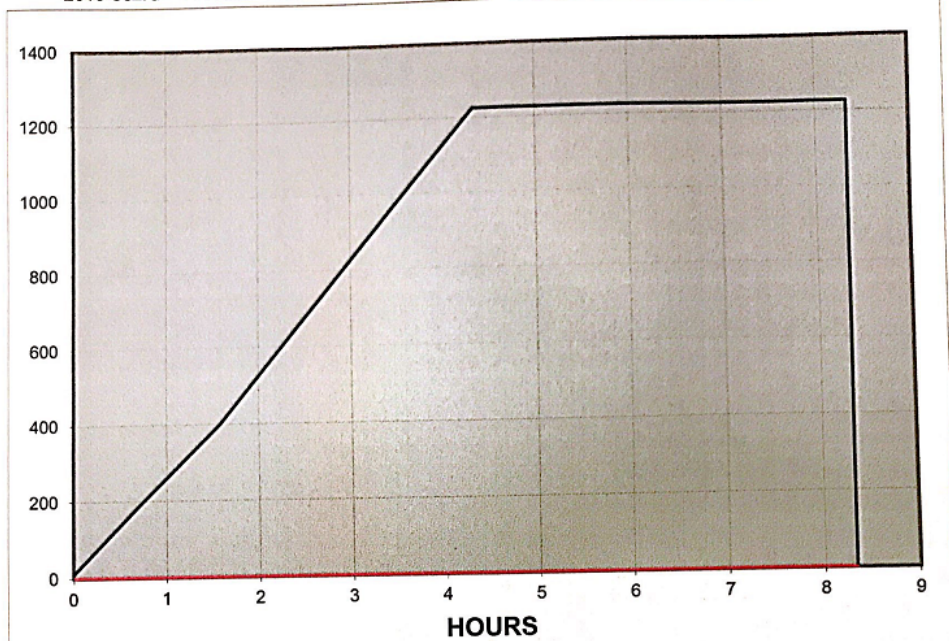
Step	Rate	Temp	Hold		H2	Ar		N2		CO	CH4	Press.		Total		
	dgr/m	dgr	m	p	nl/h	nl/h	0/1	nl/h	0/1	nl/h	nl/h	mBar	type	d	h	m
1	4.00	205	0	0	0	0	0	0	0	0	0	0	0	0	0	46
2	4.00	400	0	0	0	0	0	0	0	0	0	0	0	0	1	35
3	5.00	1225	240	0	0	0	0	0	0	0	0	0	0	0	8	20
4	0.00	0	0	0	0	0	0	0	0	0	0	0	0	0	0	0
5	0.00	0	0	0	0	0	0	0	0	0	0	0	0	0	0	0
6	0.00	0	0	0	0	0	0	0	0	0	0	0	0	0	0	0
7	0.00	0	0	0	0	0	0	0	0	0	0	0	0	0	0	0
8	0.00	0	0	0	0	0	0	0	0	0	0	0	0	0	0	0
9	0.00	0	0	0	0	0	0	0	0	0	0	0	0	0	0	0
10	0.00	0	0	0	0	0	0	0	0	0	0	0	0	0	0	0
11	0.00	0	0	0	0	0	0	0	0	0	0	0	0	0	0	0
12	0.00	0	0	0	0	0	0	0	0	0	0	0	0	0	0	0
13	0.00	0	0	0	0	0	0	0	0	0	0	0	0	0	0	0
14	0.00	0	0	0	0	0	0	0	0	0	0	0	0	0	0	0
15	0.00	0	0	0	0	0	0	0	0	0	0	0	0	0	0	0
16	0.00	0	0	0	0	0	0	0	0	0	0	0	0	0	0	0
17	0.00	0	0	0	0	0	0	0	0	0	0	0	0	0	0	0
18	0.00	0	0	0	0	0	0	0	0	0	0	0	0	0	0	0
19	0.00	0	0	0	0	0	0	0	0	0	0	0	0	0	0	0
20	0.00	0	0	0	0	0	0	0	0	0	0	0	0	0	0	0
21	0.00	0	0	0	0	0	0	0	0	0	0	0	0	0	0	0
22	0.00	0	0	0	0	0	0	0	0	0	0	0	0	0	0	0